Determinants of Predictability in Multi-decadal Forest Community and Carbon Dynamics

May 6, 2020

Authors: Ann Raiho[1], Michael Dietze[2], Andria Dawson[3], Christine R. Rollinson[4], John Tipton[5], Jason McLachlan[1]

Affiliations: University of Notre Dame Biology Department[1], Boston University Department of Earth and Environment[2], Mount Royal University Department of General Education[3], The Morton Arboretum, Center for Tree Science[4], University of Arkansas Department of Mathematical Sciences[5]

Contact: ann.raiho@gmail.com

Abstract

Predictions from ecological models necessarily include five different uncertainties: demographic stochasticity, initial conditions, external forcing (i.e., drivers/covariates), parameters, and modeled processes. However, most predictions from process-based ecological models only account for a subset of these uncertainties (e.g. only demographic stochasticity). This underestimation of uncertainty runs the risk of producing precise, but inaccurate predictions. To address these limitations, we created a new generalizable ensemble state data assimilation algorithm that accommodates two common features of ecological data, zero-truncation and zero-inflation, and allows the estimation of process error and its covariance among multiple ecological variables. We then demonstrate the use of this novel algorithm by assimilating 50 years of tree-ring-estimated species-level biomass at Harvard Forest into a process-based forest gap model. Finally, we partitioned the variance in this hindcast to test long-standing assumptions in the ecological modeling community about which uncertainties dominate our ability to forecast forest community and carbon dynamics. Contrary to >40 years of research relying on stochastic forest gap models, we found that demographic stochasticity alone massively underestimated forecast uncertainty (0.09% of the total) and resulted in overconfident and biased model predictions. Similarly, despite decades of reliance on unconstrained "spin ups" to initialize models, constraining initial conditions with data led to the largest increases in prediction accuracy. Counter to conventional wisdom from modeling other Earth

system process, initial condition uncertainty declined very little over the forecast time period. Process variance, which heretofore had been difficult to estimate in mechanistic ecosystem model projections, dominated the prediction uncertainty over the forecast time period (49.1%), followed by meteorological uncertainty (32.5%). Parameter uncertainty, which has recently been the focus of the modeling community, contributed a modest 18.3%. These findings call into question much of our conventional wisdom about how to improve forest community and carbon cycle projections on multi-decadal to centennial time scales. This foundation can be used to test long standing modeling assumptions across fields in global change biology and suggests a fairly significant reorientation of the modeling community toward better initialization of models with current observations and efforts to better quantify, propagate, and reduce process error. These approaches have the potential to improve both the accuracy of ecological forecasts and our understanding of the predictability of ecological processes.

Running Head: Drivers of multi-decadal forecast uncertainty

Keywords: climate change, paleoecology, tree rings, data assimilation, ecological forecasting, forest community ecology, Tobit Wishart ensemble filter (TWEnF)

1 Introduction

Understanding how different component uncertainties contribute to the overall uncertainty in ecological forecasts has practical value for ecologists because it allows for more efficient improvement, focusing limited resources on constraining the largest uncertainties. Furthermore, uncertainty quantification has theoretical value, helping ecologists quantify, understand, and explain the predictability of different ecological processes (Dietze 2017b; Hawkins and Sutton 2009; Cox and Stephenson 2007). Until recently, ecology lacked both the tools for including a full suite of uncertainties in complex, real-world models and a unified framework for partitioning among those uncertainties, forcing ecologists to make assumptions about which aspects of uncertainty dominate, based on qualitative evaluations or conventional wisdom. Quantitatively partitioning predictability into component uncertainties can test these long-standing assumptions in a variety of ecological fields. In models of community and population ecology, the components of uncertainty are: demographic stochasticity, internal state (i.e., initial conditions), external forcing (i.e., drivers/covariates), parameters, and modeled processes (Box 1).

These uncertainties play a role in the predictions generated by all ecological models, but to make this more concrete consider the long history of forest gap modeling in ecology (Botkin et al. 1972; Solomon et al. 1980; Pacala et al. 1993; Post and Pastor 1996). The stochasticity in discrete demographic processes, such as mortality and recruitment, has been assumed to be the dominant driver of uncertainty in forest gap

models, representing possible forest development responses to disturbance (Smith et al. 2001). While the addition of demographic stochasticity in the 1980s and 1990s represented a substantial advance in modeling forest processes (Bugmann, 2001), it is often the only source of uncertainty accounted for in forest gap models. We surveyed forest gap models reported in the literature in the last 10 years (2008-2018) that were used explicitly for forecasting. In all 15 papers, we found demographic stochasticity (Fischer et al. 2015, 2014, 2016; Gutiérrez et al. 2016; Morin et al. 2014; Sun et al. 2018; Taylor et al. 2017; Boulanger et al. 2018; Foster et al. 2017; Chauvet et al. 2017; Rödig et al. 2017b,a, 2018) was included, but only one paper accounted for any other type of uncertainty. Gutiérrez et al. (2016) incorporated parameter, meteorological, and initial condition uncertainty but omitted process uncertainty. By contrast, weather forecasts are dominated by initial condition uncertainty (Lorenz, 1963) and constraining this uncertainty has led to large increases in weather forecasting accuracy (Rabier et al. 1996). However, initial conditions in terrestrial ecosystem projections are often not constrained by data because long-term data on both above and below ground carbon pools are difficult to obtain (Todd-Brown et al. 2013). Instead of data-derived initial conditions, models are frequently 'spun-up' to steady-state in a manner that is unconstrained by data, and rarely accommodates or propagates uncertainties, under the implicit hypothesis that projections are insensitive to these assumptions (Sitch et al. 2003). Indeed, other Earth system sciences have found initial conditions uncertainties are often small and decay quickly with time (Bonan et al. 2018; Cox and Stephenson 2007). As an alternative hypothesis, the stand-level dynamics of succession, the landscape-level patch mosaic dynamics of disturbance and dispersal, and the slow accumulation of soil carbon are processes that play out over centuries to millennia, creating the possibility that even large-scale models may remain sensitive to their initialization over long periods (Watt, 1947; Jenny, 1941).

In contrast to initial conditions and internal stochasticity, some have hypothesized than external forcings dominate the predictability of vegetation (Luo et al. 2015). It is clear that external drivers are important for large scale vegetation changes (Bonan 2015), and that driver uncertainty is important to understand as climate predictions become increasingly uncertain in the future (e.g. centennial time scales), but driver uncertainty has been found to be less important at short time scales (Dietze 2017b). It remains unclear what the relative contribution of driver uncertainty is on multi-decadal timescales.

Parameters have recently been the dominant focus of calibration and uncertainty studies in terrestrial ecology (Fischer et al. 2019; Fisher et al. 2019; Fer et al. 2018; Reichstein et al. 2019; Raczka et al. 2018), as process-models often have large numbers of parameters that historically have been under-constrained by data (e.g. hand tuned). Even when constrained by data, model parameters have often been optimized to a single "best" estimate that ignores both parameter uncertainties and the common tendency for parameters to trade-off with one another (i.e. parameter covariances). Model projections without confidence intervals, which

propagate parameter uncertainty, remain the norm in the process-modeling community despite confidence intervals long being standard practice in other forms of statistical modeling and forecasting. Constraining both climate drivers and parameters with data has greatly improved model performance (Fer et al., 2018). That said, parameter uncertainty tends to decline asymptotically as data volumes increase (Dietze 2017b). Moving toward constraining parameters with data has altered ecologists perspective on what contributes most to model uncertainty (Clark et al., 2001; Dietze, 2017a). After parameter uncertainty is constrained and accounted for, it may be that parameters are overemphasized when model processes are incorrect, incomplete, or biased. Accounting for process uncertainty in a way that partitions out observation error has been shown to be necessary for generating calibrated estimates of environmental state variables and for understanding the accuracy of ecological mechanistic models in general (Cressie et al. 2009; Wikle 2003; Clark and Bjørnstad 2004). Despite this finding, process variance is rarely included in process models because robust methods for estimating process variance, and partitioning this out separately from observation error, have yet to be developed for computationally-intensive models.

Variance partitioning has been gaining use in ecology as a means to understand the large variability in many long-term predictions (e.g., the global terrestrial carbon cycle Friedlingstein et al. 2014). However, existing analyses of ecosystem predictability have only considered subsets of potential uncertainties (Lovenduski and Bonan 2017; Medlyn et al. 2015; Hewitt et al. 2016; Friend et al. 2014; Piao et al. 2013; Poulter et al. 2010; Nishina et al. 2015; Alexander et al. 2017), making it difficult to determine which uncertainties dominate and how to focus efforts to improve prediction. Furthermore, terrestrial ecosystem modelers frequently focus on partitioning variability in physiological processes over daily to annual time steps (Hui et al. 2003; Medvigy et al. 2010). This leads terrestrial modelers to focus on aspects of variance that have greater relevance over shorter time scales, in turn, potentially biasing long-term predictions. The terrestrial ecosystem modeling community has begun to advocate for including processes that are relevant over long time scales such as forest life history and stand development (Fisher et al. 2018). These forest community models contain complex demographic processes that have been hypothesized to be vital to improving long-term terrestrial ecosystem predictability (Fisher et al. 2018; Thuiller et al. 2008). But, a quantification of process variance's contribution to total uncertainty has not been completed, so it is difficult to determine how these advancements will contribute to improved forecast accuracy.

In this paper, we develop a novel sequential state data assimilation methodology for estimating process variance associated with ecological models, which is then used as part of a larger uncertainty partitioning analysis. State data assimilation is used in many disciplines to constrain estimates of a system's current and future state variables (e.g., abundance, composition in ecology) based on a forecast-analysis cycle. First, a probabilistic forecast is made by propagating the uncertainties discussed earlier through a mathematical

model. Next, this forecast is compared with new data. The forecast and the new data are then fused in a Bayesian analysis that produces an updated estimate of the state of the system (i.e., initial conditions for the next forecast-analysis step). This updated estimate is a compromise between the forecast and data. Traditional sequential data assimilation approaches assume that the process error matrix is known (Kalman, 1960), or that it is proportional to observation error (Anderson et al., 2009), neither of which is realistic for ecological systems. To address this limitation, we extend existing approaches to incorporate an estimate of the process variance (i.e., the difference between the true state of the system and the forecast). During the analysis step, there is a valuable opportunity to evaluate models by looking at biases between the model and the data and/or looking at the estimate of process variance and covariance between state variables. These steps are repeated with each new set of data to continually assess model performance. This cycle has been an important method for improving forecasting in other fields (Anderson 2001; Niu et al. 2014; Williams et al. 2005; Dietze 2017a).

Beyond methodological improvements, our objective is to empirically test long-standing assumptions about how different sources of uncertainty affect predictions of long-term forest stand development. We do this by applying our state data assimilation algorithm to assimilate 50 years of species-level aboveground biomass data at Harvard Forest in a well-established forest gap model (LINKAGES, Post and Pastor 1996). We then determine the most important sources of uncertainty affecting our ability to predict forest structure and composition over long time periods. These analyses will provide a roadmap for estimating and partitioning uncertainties across a wide range of ecological model types and a broader understanding of the limits to predictability across ecology more broadly.

This box gives more background on each type of uncertainty in ecological process models.

- **Internal demographic stochasticity** - Demographic stochasticity refers to the variability in population growth arising from random sampling of birth and deaths. Demographic stocasticity has been found to be important when predicting small or declining populations (Lande 1993; Goodman 1987). Forest gap models were initially created to simulate demographic stochasticity explicitly (JABOWA/FORET, (Botkin et al., 1972)).
- **Internal State (Initial conditions)** - Initial condition uncertainty is the uncertainty associated with the initial state of a system. For example, the number, type, and size of trees in a plot at the start of a model run. Initial conditions have been found to be particularly important in weather forecasting, because the environmental process itself is chaotic (Lorenz 1963), and in some ecological systems (Massoud et al. 2018). For ecological systems with stabilizing feedbacks this uncertainty tends to decline exponentially with time, but many ecological systems have long memory and therefore slow decay (Peterson 2002; Padisak 1992; Ogle et al. 2015). While initial conditions variance decreases over time in most ecosystem models, there may still be a significant amount of uncertainty that can be assigned to initial conditions (Alexander et al. 2017).
- **External Forcing (Drivers / covariates)** - Driver and covariate uncertainty is typically the uncertainty around external environmental forcings like temperature and precipitation. Model input drivers or model covariates are increasingly uncertain over longer time periods. For example, the weather predictions for tomorrow are much more certain than the predictions for 10 years from now. This will tend to cause both the absolute uncertainty in an ecological forecast to increase over time and the proportion of that variate attributable to drivers (Lovenduski and Bonan 2017; Bonan et al. 2018). Drivers and covariates have been shown to cause large variation among terrestrial ecosystem model predictions (Zaehle et al. 2005; Luo et al. 2015; Bonan 2015).
- **Parameter** - Parameter uncertainty arises because of our imperfect knowledge about the parameters in a model's equations. Parameter uncertainties can be estimated by calibrating models to experimental or observational data (LeBauer et al. 2013; Fer et al. 2018), but are often fixed to single values in terrestrial ecosystem models. Including parameter uncertainty is becoming more common, has been shown to improve model predictions (MacBean et al. 2015), and has been shown to increase over time in overall model uncertainty importance (Dietze 2017b).
- **Process** - Model process uncertainty is a measure of the ability of the model structure to predict the latent "true" state of the system after accounting for observation errors in the data. Without an estimate of process variance it is difficult to determine model completeness. This would be analogous to predicting with a regression model without considering its R^2 or RMSE. Process uncertainty is not typically explicitly estimated for process-based ecosystem models, as simple estimates of residual error do not partition out observation error or account for the dynamic (time-series) nature of process error (Joos et al. 2001; Knorr and Heimann 2001; Smith et al. 2001; Huntingford et al. 2008).

2 Materials and Methods

2.1 Study site and data sources

We conducted all model exercises at Harvard Forest in Petersham, MA, USA. Harvard Forest was established in 1907 as a forestry research facility. In 1988, Harvard Forest became a long-term ecological research station (LTER) to research how landscape history and past and present forest dynamics affect future changes both

at Harvard Forest and more broadly across the region (Foster and Aber 2006). The forest is at the edge of the northern hardwood and oak-hickory ecotone. The species we focused on in this forest are red oak (*Quercus rubra*), red maple (*Acer rubrum*), yellow birch (*Betula alleghaniensis*), American beech (*Fagus Granifolia*), and eastern hemlock (*Tsuga canadensis*). Red oak is the dominant species, and red maple is abundant in the understory at Harvard Forest. We chose Harvard Forest because, while it is one of the most well studied temperate forests on Earth, ecologists still struggle to constrain uncertainty around predictions about how the forest will respond to changing climate (Keenan et al. 2012).

There were four data streams used in these analyses. First, for model calibration, we used biomass estimates from the Harvard Forest Environmental Measurement Station (EMS) Eddy Flux Tower (Munger W 2018). Biomass was estimated from diameter a breast height (DBH) measurement that have been collected annually since 1994. Allometric models were applied at the species level using the Predictive Ecosystem Analyzer (PEcAn) allometry module (`https://github.com/PecanProject/pecan/tree/master/modules/allometry`). We also used data from Harvard Forest Data Archives to constrain LINKAGES parameters; this will be discussed in more detail in last paragraph of the section 2.1.1. The second data type was forest inventory and tree ring data collected from the Lyford plots at Harvard Forest (Dye et al. 2016). Lyford plot tree rings were collected in 2011. Annual species aboveground biomass and aboveground biomass increment were estimated from 1930 to 2011 using a Bayesian hierarchical model to incorporate allometric and cross dating uncertainty. We only used aboveground biomass estimates from 1960 onward in our analysis because these estimates incorporate known mortality events from stand census records between 1960 and present. The third dataset incorporated into this analysis was an ensemble of meteorological drivers (n=89) derived by probabilistically downscaling meteorological variable (temperature and precipitation) from global circulation models used in the Climate Model Intercomparison Project 5 (CMIP5) using a North American Land Data Assimilation System (NLDAS) training dataset (0.125 degree, hourly resolution), spanning from January 1979 to present (Xia et al. 2012). We used this met product instead of local meteorological data to generate a realistic representation of what driver uncertainty would be when making predictions across the larger landscape and to be consistent with data assimilation runs being conducted by the Paleoecological Observatory Network (PalEON) (Rollinson et al. 2017). We derived average monthly temperature and precipitation from these drivers to use as model specific drivers. The final dataset we used are pre-calculated meteorological ensemble weights, applied to our downscaled meteorological drivers, based on information from the North American Drought Atlas (Cook et al. 2010) and Mann et al. (2009). More information about these data sources and how they were processed can be found in the supplemental materials section 5.1.

2.1.1 Ecosystem model

All of the following model analyses took place within the Predictive Ecosystem Analyzer (PEcAn, `pecanproject.org`). PEcAn's mission is to develop and promote accessible tools for reproducible ecosystem modeling and forecasting (Dietze et al. 2013). The specific modules we used within PEcAn, besides the basic workflow, were: allometry, sensitivity analysis, and state data assimilation. Furthermore, outputs were saved in a standard NetCDF format to be comparable to future modeling studies.

Forest gap models have been used for about 50 years to predict forest stand development and ecosystem dynamics (Bugmann 2001). Forest gap models typically focus on demographic processes, including growth, recruitment, and mortality, that are functions of environmental factors such as available soil nitrogen, soil moisture, light, or growing season length. Forest gap models have been validated in many contexts (Scheller and Mladenoff 2004; Lindner et al. 1997; Bugmann et al. 1996; Solomon 1986), and are used by scientists and land managers to predict future forest stand composition and structure, but they are typically used without uncertainty estimates so it can be difficult to assess which uncertainties affects long-term predictability.

LINKAGES is a forest gap model that was first created by Post and Pastor (1996) to link forest above-ground demographic processes with below ground biogeochemical processes during forest stand development (Figure 1). The model works on an annual time step and uses species level representation for model parameters. LINKAGES tracks each individual tree's diameter at breast height (DBH), age, and number of years with unfavorable growing conditions. Every year, LINKAGES calculates four growth factors using environmental conditions: soil moisture, growing degree days, available light, and available nitrogen. Meteorological drivers are used to calculate available soil moisture and growing degree days, while the available light and soil nitrogen growth multipliers are calculated using model internal functions and information about individuals and carbon pools in the plot. According to Liebig's law of the minimum, the lowest growth factor is used for each species and the DBH's are incremented according to that growth factor. For example, if the maximum growth increment parameter for red oak is 1 cm per year and the lowest growth factor is 0.2, then, the growth increment for red oak that year is 1 cm x 0.2 = 0.2 cm.

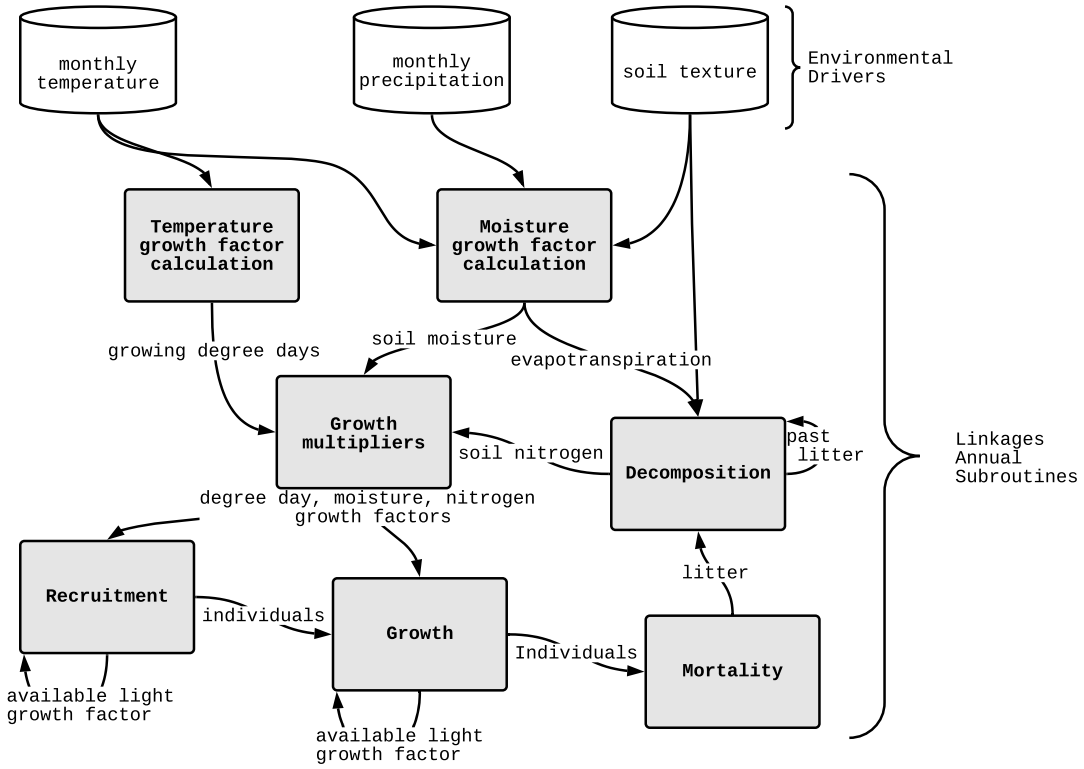

Figure 1: Conceptual diagram of the forest gap model LINKAGES (Post and Pastor 1996). Environmental driver data is used by subroutine temperature, moisture, and decomposition to calculate annual growth factors for growing degree day, soil moisture, and soil nitrogen in the growth multipliers subroutine. Growth multipliers subroutine calculates species specific growth factors using species specific parameters (highlighted in blue, acronyms available in supplemental materials figure 11). These annual growth factors along with diameter at breast height (DBH), age, and growing status of each individual are input into recruitment, growth, and mortality subroutines. Within the recruitment, growth, and mortality subroutines individual DBH, age, and growing status are incremented and individuals can be recruited or be removed (mortality) based on site conditions. Available light growth multipliers are calculated for each individual during the growth subroutine. Litter pools are saved year to year and contribute to available nitrogen and soil nitrogen growth factors calculated in the decomposition subroutine.

There are 21 parameters per species in LINKAGES. We used Harvard Forest field measurements to improve parameter representation and incorporate parameter uncertainty in the following PEcAn workflow (LeBauer et al. 2013). First, we defined Bayesian prior distributions for each parameter. We began by giving each parameter an uninformative prior distribution with a mean based on the default LINKAGES parameterization. To identify the parameters most needing constraint and reduce the dimensionality of subsequent parameterization efforts, we conducted a one-at-a-time parameter uncertainty analysis. Using a Bayesian meta-analysis (LeBauer et al., 2013), we were able to constrain specific leaf area (SLA) for each species with trait data from the (BETY) database (LeBauer et al., 2018), and allometric and recruitment parameters with information from Catovsky S (2000), Dietze et al. (2008), and Sullivan et al. (2017). All

parameter prior distributions and the uncertainty analysis results can be found in the supplemental materials section 6.

2.2 State data assimilation

2.2.1 General description

State data assimilation (SDA) is a method used to update the state variables in a modeled process based on observations, in a way that accounts for the uncertainties in both the model and the data. Here, we used sequential SDA which means that our predictions were updated iteratively at every time step. One of the most common applications of sequential SDA is weather forecasting. In weather forecasting, sequential SDA is used to update weather state variables, like temperature and humidity, when weather data become available. Here, our analysis was a hindcast, because we were running the model from 1960 to 2010, but to the extent possible our model was being run as one would run a forecast. Sequential SDA occurs in three steps following the forecast-data cycle (Dietze 2017a). First, an ensemble of model runs (n=89) was used to make a probabilistic prediction into the next year. Here, the state variables of interest were the biomass of five tree species (red maple [*Acer rubrum*], red oak [*Quercus rubra*], yellow birch [*Betula alleghaniensis*], American beech [*Fagus granafolia*] and hemlock [*Tsuga canadensis*]) and soil carbon amount. Second, the state variables were adjusted using the data from the tree ring estimated biomass. Finally, the model was restarted with new state variable quantities using the updated information.

A common method used for sequential SDA is the ensemble Kalman Filter (EnKF, (Evensen, 2009)). The ensemble Kalman Filter is itself a generalization of earlier approaches, which assumed the process model was either linear (Kalman Filter, Kalman 1960) or could be approximated using a linear tangent (extended Kalman Filter). The EnKF aims to relax these linearity assumptions by approximating the forecast probability distribution with an ensemble of model runs. During the analysis step the EnKF assumes that the forecast and observations both follow multivariate Normal distributions, which allows it to have an analytical solution and operate efficiently. However, the EnKF treats both the observation error and process error as known. This assumption is often reasonable for observations, where uncertainties are reported or can be estimated, but it is infeasible for ecological models to assume that the process error is known before the difference between the model and data is observed. In addition to the process error assumption, the Normal assumption of the Kalman analysis is also often violated with ecological data. For example, many ecological variables have clear upper and/or lower bounds, with zero-bound data being particularly common. In our example, both biomass and soil carbon cannot sensibly be negative. Furthermore, ecological data and models are also often zero-inflated (Martin et al. 2005; Hall 2000), where a species might be locally absent

from some census plots but found in others. Likewise, a species might go locally extinct in individual model ensemble members but survive in others.

2.2.2 Tobit Wishart Ensemble Filter (TWEnF)

To confront the obstacles with the EnKF, we created a Tobit Wishart Ensemble Filter (TWEnF). The TWEnF can estimate process variance over time and overcomes the assumption that the forecast is Normal by mapping the forecast state variables to normalized censored space (Figure 2). The TWEnF is similar to the EnKF, but in the TWEnF we added a latent state vector that accounts for added process variance. Furthermore, instead of solving the analysis analytically like the EnKF, we estimated the mean analysis vector and covariance matrix with MCMC. We also leverage a Tobit transformed likelihood, which works like a censored regression and allows us to use non-Normal forecasts that are zero-bound, and possibly zero inflated, for a state variable. This also allowed us to weight the likelihood, which in this application we are using to account for the known ensemble meteorological driver weights (Papadakis et al. 2010).

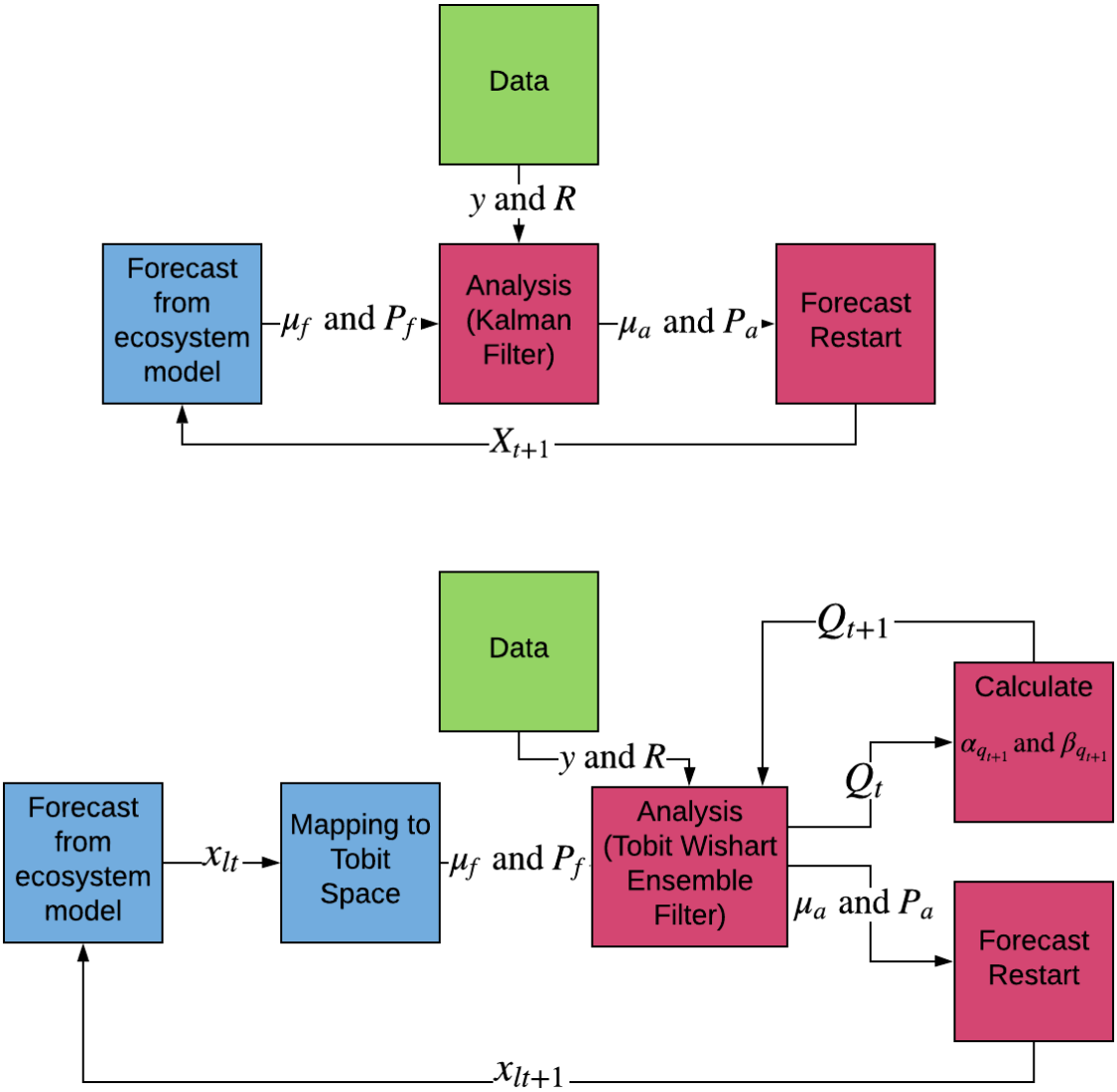

Figure 2: Conceptual diagram of the workflow involved in both the ensemble Kalman filter (EnKF, top) and the Tobit Wishart ensemble filter (TWEnF, bottom). Each method works in a forecast cycle (Dietze 2017a) where the model forecast (blue) is updated by the data (green) into an analysis (pink) that is used to restart the forecast for another time step. The difference between these filters is that the TWEnF is generalized for non-Normal forecasts and can also estimate the process covariance matrix over time. Let y be data mean, R be data covariance, μ_f be forecast mean, P_f be forecast covariance, μ_a be mean analysis, P_a be analysis covariance, Q_t be process covariance matrix at time t, and x_{lt} be the left censored model ensembles.

Before performing each analysis step, we first have to calculate the forecast mean and covariance. In the traditional EnKF, this is the ensemble sample mean ($\boldsymbol{\mu}_f$) and covariance ($\boldsymbol{P}_f$), but because we applied the Tobit transformation, we estimated $\boldsymbol{\mu}_f$ and $\boldsymbol{P}_f$ with a Normal-inverse-Wishart as follows

$$
\begin{aligned}
z_{ij} &= \begin{cases} 0 & x_{ij} \leq y_L \\ 1 & x_{ij} > y_L \end{cases} \\
\boldsymbol{x}_i &\sim \mathrm{N}(\boldsymbol{\mu}_f, \boldsymbol{P}_f)^{w_i} \\
\boldsymbol{\mu}_f &\sim \mathrm{N}(\boldsymbol{\mu}_0, \boldsymbol{\Sigma}_0) \\
\boldsymbol{P}_f &\sim \mathrm{Inv-Wishart}(\boldsymbol{S}, \nu),
\end{aligned}
$$

where $\boldsymbol{\Sigma}_0$ and S are prior covariances (on the forecast mean and covariance respectively), ν is the number of elements in the forecast mean vector ($\boldsymbol{\mu}_f$), $\boldsymbol{\mu}_0$ is prior mean vector, $\boldsymbol{x}_i$ is a vector of predicted state variables for each forecast ensemble member i, z_{ij} is an indicator variable indicating which state variable (j) of each ensemble member (i) is outside of the truncated space, and y_L is the left truncation for the Tobit, which equals 0 in our case. Finally, w_i is the known weight associated with each of the ensemble members based on an a priori analysis of the meteorological drivers described in the supplemental materials section 5.1. We fit this model in the R version 3.4.4 computing environment using the 'nimble' package version 0.8.0 (Team et al. 2017; de Valpine et al. 2017) assuming vague priors. We used a user defined 'toggle' sampler that samples $\boldsymbol{x}_i$ with a random walk sampler when $z_{ij} = 0$. We also wrote a user defined conjugate sampler for $\boldsymbol{P}_f$ to incorporate ensemble weights w_i. These are available in the PEcAn GitHub repository (`https://github.com/PecanProject/pecan`).

With $\boldsymbol{\mu}_f$ and $\boldsymbol{P}_f$ now in hand, the TWEnF analysis step is based off the EnKF, but in the TWEnF we added a latent state vector ($\boldsymbol{x}_l$) that accounts for added process variance and non-Normal errors. Like the previous step, we begin with a Tobit transformed likelihood (Eqn. 1), but this time we are using the Tobit to account for zero truncation and zero inflation in the data, rather than the forecast. The following TWEnF was fit at every time step.

$$\boldsymbol{y} \sim \begin{cases} \text{MVN}(\boldsymbol{x}_l, \boldsymbol{R}) & > y_L \\ y_L & \leq y_L \end{cases} \tag{1}$$

$$y_j = \begin{cases} y_j^* & \text{if } y_j^* > y_L \\ y_L & \text{if } y_j^* \leq y_L \end{cases} \tag{2}$$

$$\boldsymbol{x}_l \sim \text{MVN}(\boldsymbol{x}_f, \boldsymbol{Q}) \tag{3}$$

$$\boldsymbol{x}_f \sim \text{MVN}(\boldsymbol{\mu}_f, \boldsymbol{P}_f) \tag{4}$$

$$\boldsymbol{Q} \sim \text{Inv} - \text{Wishart}(\boldsymbol{\Omega}_q, \beta_q), \tag{5}$$

where $\boldsymbol{y}$ is the mean data vector calculated from the posterior of the tree ring aboveground biomass data product, $\boldsymbol{R}$ is the observation error covariance calculated from the posterior draws of the same data product, $\boldsymbol{x}_l$ is the latent model state that is estimated from the forecast ensemble mean $\boldsymbol{x}_f$ and process covariance $\boldsymbol{Q}$. Let $\boldsymbol{\Omega}_q$ and β_q be the prior shape parameters for the process covariance that are estimated over time, as described in the next paragraph. This model was also fit in using 'nimble'. We used a random walk block sampler to fit $\boldsymbol{x}$ and $\boldsymbol{x}_f$ where there are data from $\boldsymbol{y}$ (Roberts and Sahu, 1997). We used slice samplers for $\boldsymbol{x}$ and $\boldsymbol{x}_f$ where there are no data from $\boldsymbol{y}$ (Neal, 2003). In our case, we also used a slice sampler for the soil carbon pool because we do not have data directly informing this state variable. We again used the toggle sampler for $\boldsymbol{y}$ that contain zeros and we used a conjugate (Gibbs) sampler for $\boldsymbol{Q}$.

From the MCMC posterior draws of $\boldsymbol{x}_l$, we calculate the analysis mean ($\boldsymbol{\mu}_a$) and covariance ($\boldsymbol{P}_a$). The analysis mean and covariance are then used, as they would be in a ensemble adjustment filter (Anderson 2001), to "nudge" the forecast ensemble members to have the correct posterior mean and covariance. After the adjustment, we restarted each ecosystem model ensemble member with an updated state vector. The specific LINKAGES restart scripts are described in Supplemental Section 7. We updated the estimate of the process covariance ($\boldsymbol{Q}_t$) every time step by updating the shape parameters of the Inverse Wishart distribution as follows

$$\Omega_{q_{t+1}} = \bar{Q}_t \beta_{q_{t+1}} \tag{6}$$

$$\beta_{q_{t+1}} = E\left[\frac{\Omega_{rc}^2 + \Omega_{rr}\Omega_{cc}}{var(\Omega_{rc})}\right]_t, \tag{7}$$

where Ω is the process precision to the process covariance Q_t and r and c represent the rows and columns of the process precision matrix. In this step of the analysis, $\bar{Q}_t$ is the posterior mean estimate of Q_t from the

TWEnF. We assessed convergence at every time step using the Gelman-Rubin convergence diagnostic with the 'coda' package (Gelman et al. 1992; Plummer et al. 2006). Our workflow was restarted with different initial conditions if Gelman-Rubin diagnostics were greater than 1.01 for more than two monitored variables.

All data for analysis, analysis workflow scripts, and post processing scripts can be found at PEcAn workflow IDs 1000009667, 1000009397, and 1000010510. ID 1000009667 contains the bulk of the variance partitioning output. ID 1000010510 and 1000009397 contain the model runs for understanding the effects of updating the parameters with prior information. Furthermore, the analysis scripts are available as part of the assim.sequential package within PEcAn at: `https://github.com/PecanProject/pecan/tree/develop/modules/assim.sequential`.

2.2.3 Diagnostics

We look at several diagnostics for every state variable to assess the ability of the TWEnF to assimilate tree ring estimated biomass into LINKAGES. Specifically, we defined the model error as the forecast minus the data and the update as the forecast minus the analysis (Dietze 2017a). While the error is analogous to a residual, the update diagnostic shows us how much the model needed to be adjusted every time step. Both of these diagnostics give us an indication of model bias. If the model bias is not normally centered around zero over time, we have a clue that the model may need more calibration of a specific state variable. If the model bias increases or decreases over time, we would suspect that the model process behind that state variable may need to be adjusted. The direction of the model bias away from zero indicates what processes may need to be changed. For example, if the bias is increasingly positive for a specific species biomass, then we would suspect that the model is not representing mortality correctly for that species because the forecast is increasingly much larger than the analysis. Other types of diagnostics include root mean square error, correlation coefficient, and R^2 which are also used for testing the similarities and differences between the model forecast and the data (Hyndman and Koehler 2006).

By updating the state variables each time step, data assimilation allows better identification of errors made at a specific point. Traditional model diagnostics, by contrast, tend to emphasize cumulative errors. For example, a model forecasting at the current time step may be more accurate now because it was incorrect in the past, but by coincidence, the model bias has lead it to be correct at this particular time step. Similarly, a model that makes a mistake early on may continue on the wrong trajectory, even if it represents subsequent processes correctly, leading an otherwise good model to have large error statistics. This error discrepancy can be misleading about what may actually be wrong with the model.

2.3 Hindcasting uncertainty scenarios

Partitioning variance is a method for quantifying which aspects of uncertainty are driving model precision. Variance partitioning has the potential to show ecologists where to focus efforts to constrain long-term predictions, which currently are particularly uncertain (Friedlingstein et al. 2014). To partition variance, we ran model scenarios where we sequentially added five types of uncertainty. We first divided the scenarios into two initial condition types: model spin up or informed by data. Model spin up is a typical process in ecosystem modeling where the model is run for many time steps until it is determined that the state variables have reached steady state. Data-constrained initial conditions are those based on observations in the field. Here, we constrained model initial conditions with data by informing the very first time step using the TWEnF analysis, but not using data assimilation thereafter.

We ran two sets of scenarios to partition the effect of spin up initial conditions (Scenarios A1-4) versus data constrained initial conditions on forecast variance (Scenarios B1-4). In each scenario batch, initial condition uncertainty was the first type of uncertainty added to the default ecosystem model. The default version of LINKAGES's only source of variability was demographic stochasticity. So, the default version of LINKAGES plus initial condition uncertainty were scenarios A1 and B1 in this analysis. We then added the following uncertainties sequentially: parameter (A2 and B2), meteorological (A3 and B3), and process uncertainty (A4 and B4) (Table 1). Parameter uncertainty was added by running each ensemble member with a different parameter set, sampled from the calibration posteriors, while in the default run all ensemble members were run at the posterior means. Similarly, to incorporate meteorological uncertainty we ran ensemble members with samples from the meteorological ensemble versus the ensemble mean. Finally, to incorporate process error we used the final posterior mean of the process covariance (Q) from the full data assimilation run. In this scenario, runs were done leveraging the SDA workflow, stopping the model each year to add process error then restarting, but no data constraints were added during the analysis step (except for year 1 in the B1, data constrained initial conditions scenario).

Scenario	Demographic	Initial Conditions	Parameter	Meteorological	Process
A1	X	Spin Up			
A2	X	Spin Up	X		
A3	X	Spin Up	X	X	
A4	X	Spin Up	X	X	X
B1	X	Data Derived			
B2	X	Data Derived	X		
B3	X	Data Derived	X	X	
B4	X	Data Derived	X	X	X

Table 1: This table indicates which types of uncertainty are included in each scenario with an 'X.'

2.3.1 Variance partitioning

We estimated the effect of each source of variance by calculating the difference in variance between pairs of scenarios (Dietze 2017b). This is similar to analytical approximation methods (Hawkins and Sutton 2009) but our sequential approach accounted for nonlinear interactions that may affect prediction.

Our scenarios did not allow a full variance partitioning because we did not introduce each source of variance independently from the other sources of variance in all possible permutations. However, because we had two sets of scenarios: one with data derived initial conditions and one with spin up based initial conditions, we were able to calculate the covariance between data derived initial condition variance and the other components of variance ($Cov[A, B]$, eqn. 8). This calculation gives us an idea of how long lasting data derived initial conditions affect the forecast variance. As an example, we calculated the magnitude of the interaction terms with the following equation for variance between two variables P (parameters) and IC (initial conditions):

$$Var\,[P, IC] \sim Var\,[P] + Var\,[IC] + 2Cov\,[P, IC] \tag{8}$$

$$Var[A2] \sim Var[B2] + (Var[A1] - Var[B1]) + 2Cov\,[P, IC] \tag{9}$$

where we substitute $Var[P, IC]$ with the variance from scenario A2 that includes uncertainty from spin up and parameters, $Var[P]$ with variance from scenario B2 (parameters, constrained IC), and $Var[IC]$ with the difference between variance in scenarios A1 (spin up) and B1 (constrained IC) that do not include uncertainty from parameters. We used these values to solve for $Cov[P, IC]$, which is the covariance between initial condition uncertainty and the other types of uncertainty. Following similar logic, we can solve for $Cov[M, IC]$ and $Cov[Process, IC]$ using the difference between the subsequent scenario variances as the $Var[IC]$.

3 Results

3.1 Model parameterization

Default parameters resulted in both incorrect forest composition and biomass compared with Harvard Forest EMS Tower species biomass data (Figure 3 and Table 2). LINKAGES with default parameterization predicted that hemlock should be the dominant species with low total stand biomass ($\approx$ 5 kgC/m^2). The data indicated that red oak was the dominant species with higher total stand biomass ($\approx$ 15 kgC/m^2). Parameters informed from SLA meta analysis and literature review for allometric and recruitment parameters

allowed LINKAGES to better represent total forest biomass ($\approx$ 10kgC/m^2) but not species composition. Our parameter uncertainty analysis revealed that while there were some parameters that could be constrained with model calibration, the majority were not causing sufficient model sensitivity to warrant a full parameter calibration effort (See supplemental section 6.6).

	R^2	RMSE	Euclidean Distance
Default Parameterization	0.00076	4.66	10.89
Informed Parameterization	0.040	5.06	11.52

Table 2: Bias diagnostics for LINKAGES compared with Harvard Forest EMS Tower data with default and calibrated parameterizations. R^2 and root mean square error (RMSE) are calculated for total stand biomass and Euclidean distances (e.g. root square sums) are calculated between average species composition vectors over the time period 1998 to 2009.

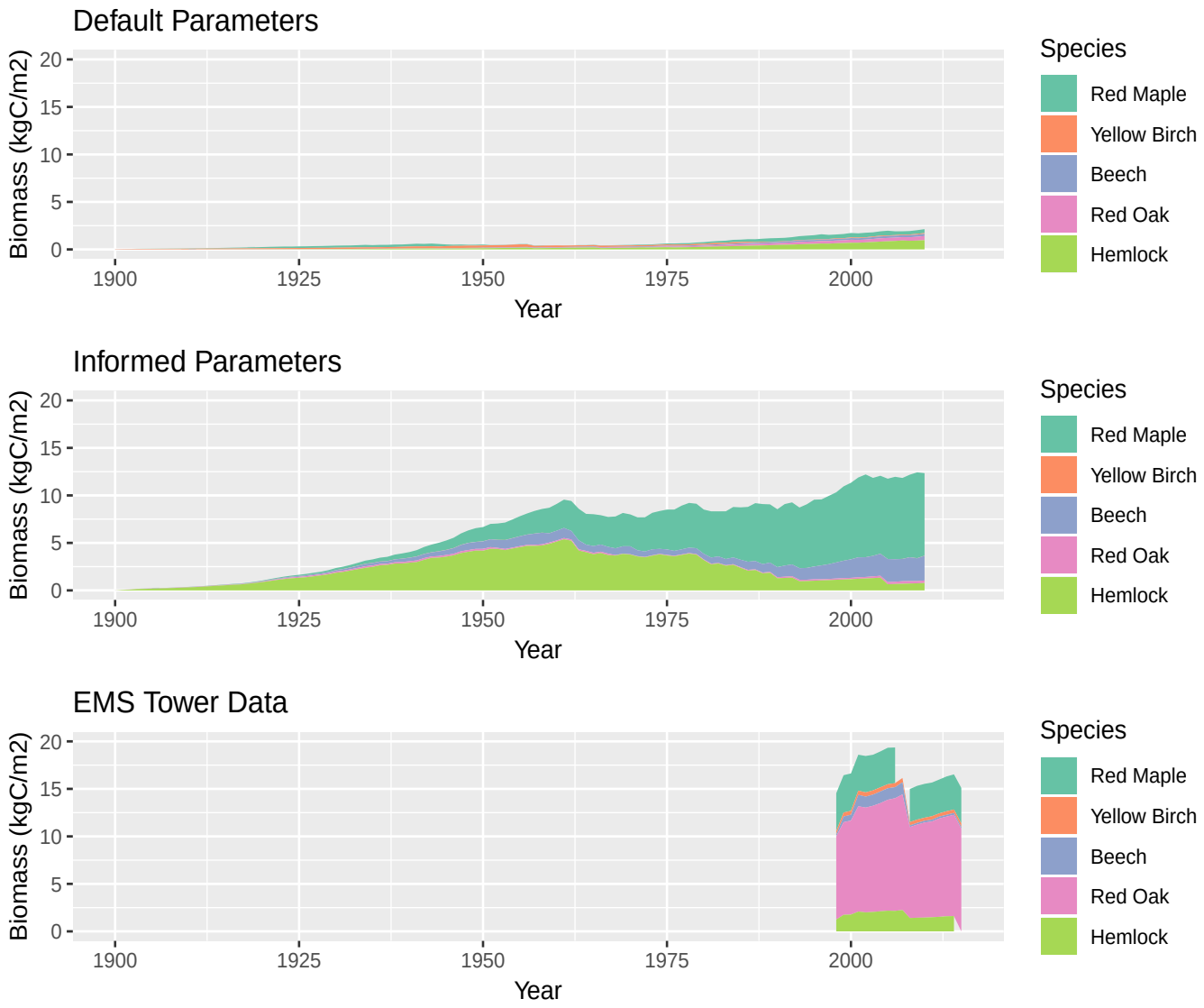

Figure 3: Cumulative time series of species level biomass from LINKAGES run with default parameters (panel 1) and parameters derived from informative priors (panel 2). We compare with data from the Harvard Forest EMS tower (panel 3).

3.2 State data assimilation

State data assimilation successfully constrained LINKAGES to produce accurate forest biomass and composition while including demographic stochasticity and parameter, meteorological, and process uncertainties (Figure 4). During time periods of increased variance in the tree ring biomass data product, our state data assimilation system adjusted to match, with increased variance in the forecast. Red oak, the most abundant species in our data, was best represented by LINKAGES with a high R^2 between the modeled red oak and the data (R^2= 0.769) (Supplemental Figure 5). As the most abundant species, red oak also had the largest

average model bias (-0.82 kgC/m^2/yr, 76% of total bias, Table 3) and largest estimated process variance among the aboveground biomass of species ($\sigma^2 = 0.25$). This bias increased over time indicating that the modeled process of red oak mortality may need adjustment. The second most abundant species was red maple that had a persistent negative bias (-0.14 kgC/m^2/yr, Supplemental Figure 2). Both red oak and red maple's negative biases are consistent with the unconstrained run (where oak and maple went locally extinct) and may suggest a need for red oak and red maple parameter calibration and/or model competitive process evaluation (Supplemental Figure 2). However, both species had low estimated process variances ($\sigma^2 = 0.25$, 0.13) indicating LINKAGES modeled representations of the two most abundant species was adequate for prediction if the process covariances were incorporated. Beech and hemlock were well represented by LINKAGES despite low abundances (beech, $R^2 = 0.796$; hemlock, $R^2 = 0.682$, Table 3). There was a consistent small negative bias (-0.04 kgC/m^2/yr) for beech and a small consistent positive bias (0.06 kgC/m^2/yr) for hemlock (Supplemental Figures 4 and 6). Yellow birch was in low abundance at the Lyford plot and this low biomass species was not well represented by LINKAGES with an R^2 of 0.274 between the modeled forecast and the data (Supplemental Figure 3). However, yellow birch bias was small (-0.01 kgC/m^2/yr) and centered around zero indicating that parameter calibration is not required (Supplemental Figure 3). Finally, soil carbon was the only state variable in our analysis unconstrained by data. Because soil carbon is unconstrained, the soil carbon pool has the highest process variance estimate ($\sigma^2 = 1.03$, Table 3), but interestingly, was not highly correlated with any particular species biomass.

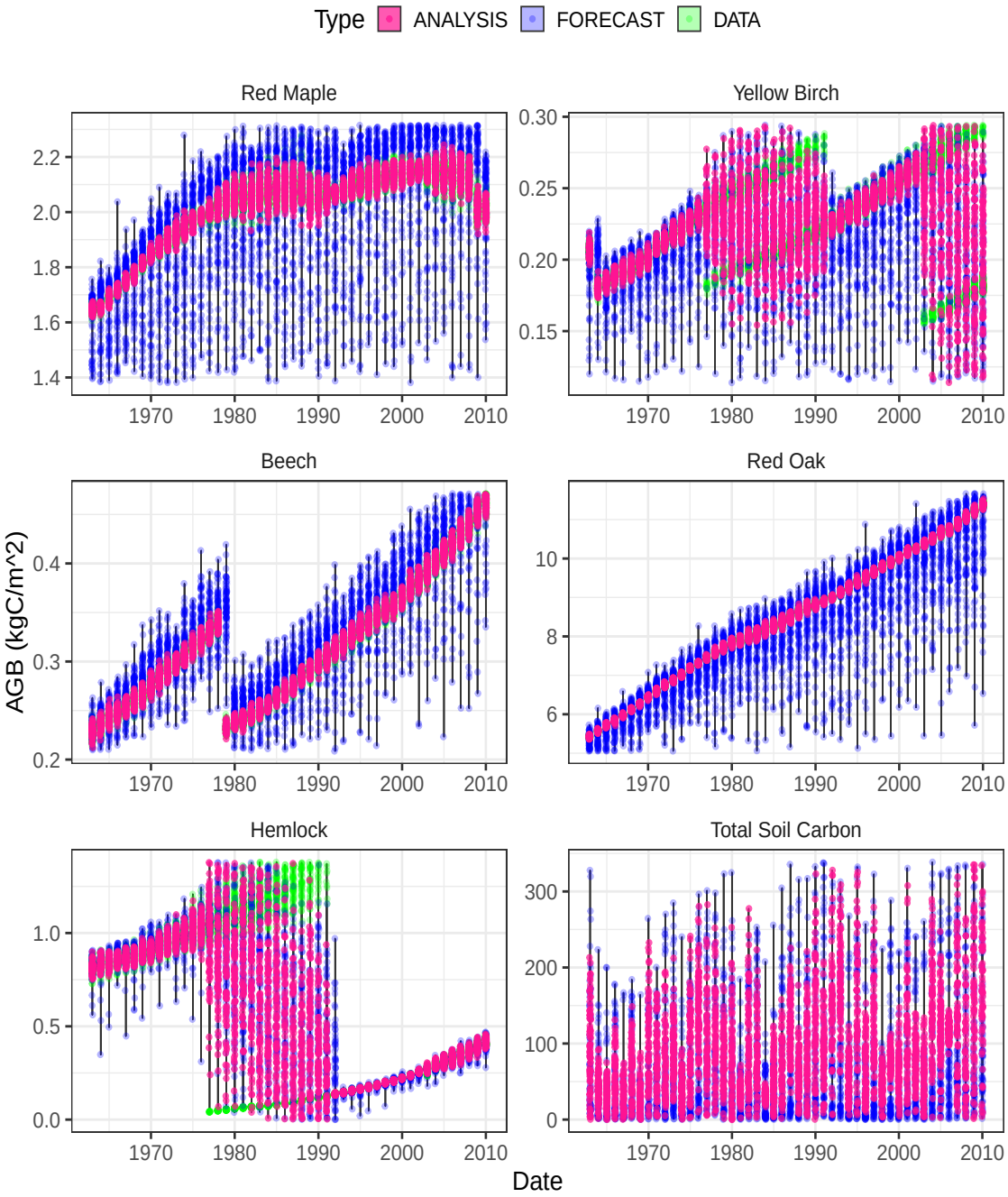

Figure 4: Species biomass time series illustrating the difference between the model forecast (blue), data (green), and analysis (pink) in LINKAGES state data assimilation of tree ring derived aboveground biomass. The green confidence intervals behind the pink and blue dots are confidence intervals of the tree ring estimated species level biomass. The black vertical lines indicate time points where data was assimilated, in this case annually between 1961 and 2010. The blue points are 89 LINKAGES forecasts of one year forward following an analysis (pink). The pink points are 89 species biomass values drawn from the estimates of average species biomass in the Tobit Wishart ensemble filter (TWEnF). The analysis points are used to restart the 89 model ensemble members. The pink points generally align with the mean of the data while the forecasts sometimes drift from the data. The data are bimodal during some time intervals between censuses because the timing of mortality events is unknown. We do not use bimodal posteriors directly but instead calculate a mean and variance to a Normal likelihood.

State Variable	Average Model Bias ($kgC/m^2/yr$)	Estimated Process Variance	Average Forecast Total Biomass ($kgC/m^2/yr$)
Red Oak	-0.82	0.25	7.55
Red Maple	-0.14	0.13	1.86
Eastern Hemlock	0.06	0.13	0.62
American Beech	-0.04	0.13	0.28
Yellow Birch	-0.01	0.09	0.22
Total Soil Carbon	–	1.03	9.83

Table 3: Model diagnostics ordered by species biomass. Average model bias is simply the average modeled minus observed annual means. Estimated process variance for each species is estimated over time using the Tobit Wishart ensemble filter (TWEnF). Average forecast total biomass is the average modelled biomass for each state variable to give a reference point for the magnitude of the estimated process variance.

The process covariance matrix was estimated over the state data assimilation time period. The increasing degrees of freedom over time was evidence that the estimation is increasingly constrained over time (Figure 5 left). The values associated with each species biomass, along the diagonal of the process covariance matrix, were estimated to be small (Table 3 column 3), indicating annual species biomass accumulation process is well represented by the ecosystem model after accounting for uncertainty in the data. Similarly, the species correlations in the process covariance matrix were estimated to be small with the most significant correlation between species being a small negative relationship between beech and red oak (correlation = -0.125, Figure 5). This suggested that while LINKAGES typically represents beech and red oak as having a positive interaction (forecast correlation = .105, supplemental materials figure 18) they were actually more neutral with one another at Harvard Forest according to the data. Soil carbon was not estimated to be highly correlated with any species biomasses in the process covariance matrix (correlations between -0.009 and .0002), but was somewhat more correlated with species biomasses in the forecast covariance matrix (correlations between -0.238 and 0.168, Supplemental Figure 8). This shows that although we were leveraging information about the species biomass to inform soil carbon indirectly through the process covariance that our analysis was not influencing the modeled processes between species biomasses and soil carbon because there is no data directly informing soil carbon. Put simply, we were depending on LINKAGES to update soil carbon given the data we were providing on species biomasses. This technique can be explored more in the future for constraining unobservable state variables with known modeled processes and corresponding covariance with observed state variables.

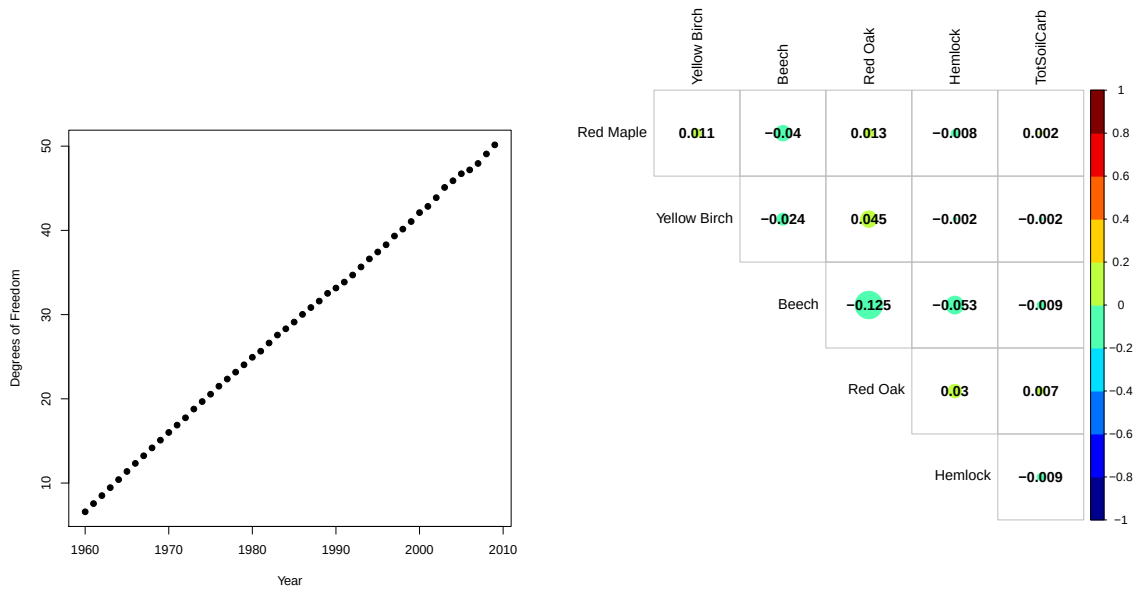

Figure 5: The left hand plot shows the degrees of freedom associated with the estimation of the process covariance. The right hand plot is a correlation diagram of the process covariance. The colors in the correlation diagram correspond to the magnitude and direction of the correlation. The diagonal variances can be found in Table 3.

3.3 Hindcasting uncertainty scenarios

Across all uncertainty scenarios, data constrained initial conditions reduced model bias and improved root mean square error. Across most uncertainty scenarios, excluding scenario A1 and B1, data constrained initial conditions lowered average forecast variance (Table 4). The default model run with only demographic stochasticity as a source of variance, with either spin up initial conditions or data derived initial conditions (Figure 6, row 1), was precise (average forecast variance = 0.102 kgC/m^2 and 1.450 kgC/m^2) compared to the actual residual error (average observation variance = 0.0719 kgC/m^2). However, the root mean square error between the hindcast and the data decreased when the initial conditions were constrained with data (RMSE = 9.81 spin up initial conditions, 4.42 data derived initial conditions). The correlation coefficient was closer to one in scenario A1 (0.934) versus scenario B1 (0.262) because the data and the spun up model both increased in biomass more linearly than the scenario with data derived initial conditions and only demographic stochasticity.

Sequentially adding uncertainties (scenarios A2-4 and B2-4) led to greatly increased forecast variance and the variance in the spin up scenarios (A) was consistently larger than the data constrained initial conditions (B, Table 4). Adding meteorological uncertainty increased variance in the spin up initial conditions (variance increased $\approx$ 170 kgC/m^2/yr) much more than the data derived initial condition scenario (variance increased $\approx$ 10 kgC/m^2/yr) (Figure 6, row 3, Table 4). Process variance increased uncertainty in the spin up initial

condition scenario (Figure 6, column 1, row 4) and to a greater extent in the data constrained initial condition scenario (Figure 6, column 2, row 4). Interestingly, adding process uncertainty reduced model bias (from -1.88 to 0.669) and increased the correlation coefficient slightly between the model and the data (from .929 to .954) in the data derived initial condition scenarios. This improvement occurred because the process covariance constrained species biomass by inducing species covariances that were not present in the model but were present in the data (Supplemental Figure 6). In these scenarios, more model ensembles had higher biomass red oak and presence of sub-canopy species hemlock and yellow birch that were less abundant in scenarios that do not include process covariance (scenarios A1-3 and B1-3).

Hindcast Diagnostic	Scenario	Demographic Stochasticity	+ Parameter	+ Meterological	+ Process
Average Model Bias ($kgC/m^2/yr$)	Spin-up IC	-9.72	-4.85	-2.89	4.090
Average Model Bias ($kgC/m^2/yr$)	Data IC	-4.07	-2.23	-1.88	0.669
Correlation Coefficient	Spin-up IC	0.934	0.972	0.968	0.966
Correlation Coefficient	Data IC	0.262	0.912	0.929	0.954
Root Mean Square Error	Spin-up IC	9.81	4.86	3.29	5.39
Root Mean Square Error	Data IC	4.42	2.35	2.01	2.00
Average Forecast Variance ($kgC/m^2/yr$)	Spin-up IC	0.103	141.0	310.0	326
Average Forecast Variance ($kgC/m^2/yr$)	Data IC	1.450	20.3	30.1	71

Table 4: Model diagnostics for hindcasting scenarios. Data constrained initial conditions reduce model bias across scenarios.

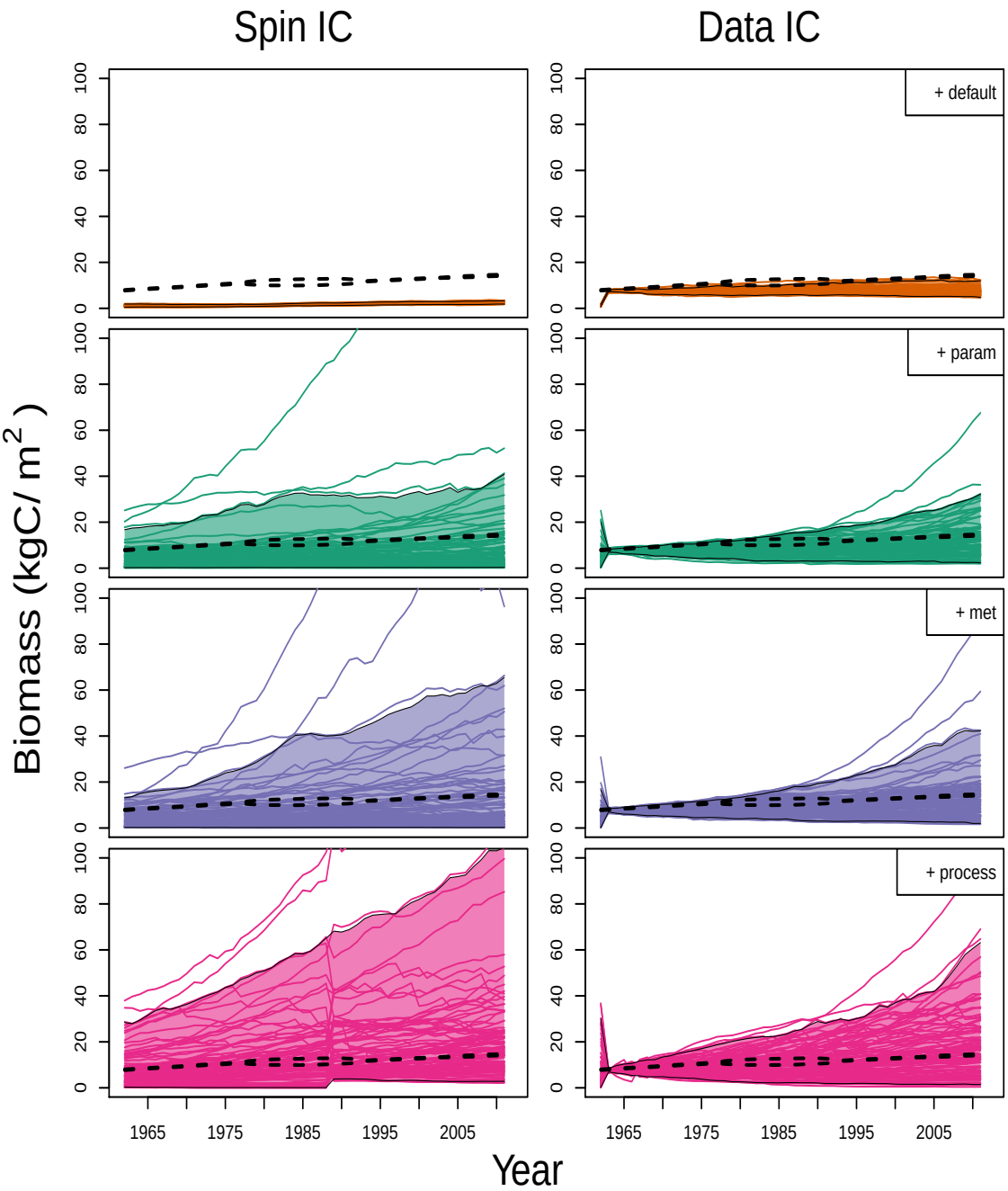

Figure 6: Individual model ensemble members overlaid with shaded 95% quantiles (outlined in black) of aboveground biomass results from each uncertainty scenario using spin up as the model's initial conditions (left) and using data to constrain the model's initial conditions (right). Default was ran with initial condition uncertainty and internal model demographic stochasticity (first row). Next, parameter uncertainty was added (second row), followed by meteorological uncertainty (third row). Finally process uncertainty estimated in the full data assimilation was added (fourth row). The dotted lines on all the plots are the 95% credible intervals of the data estimated from tree rings.

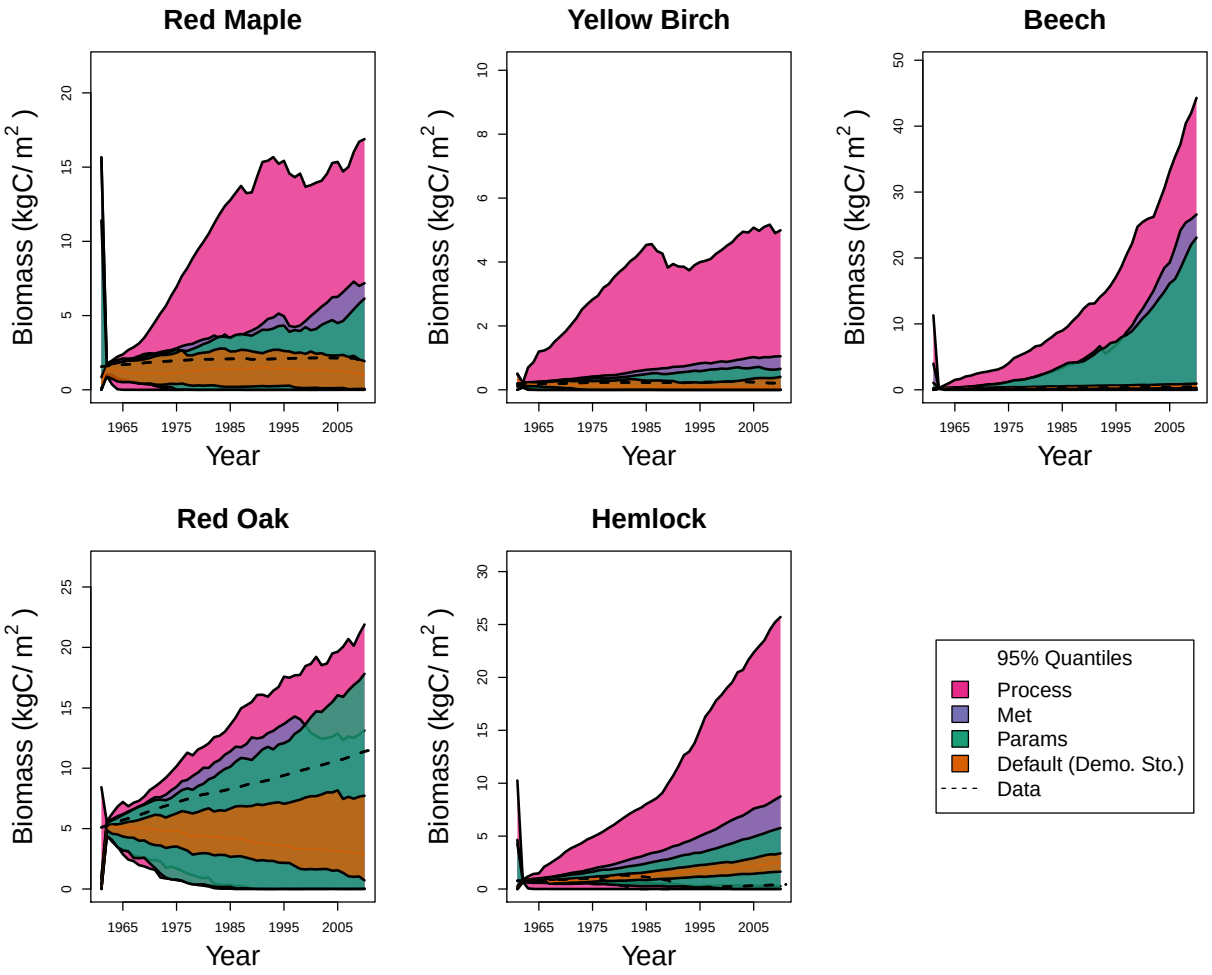

Figure 7: 95% quantiles of species level biomass over time colored by the four data constrained initial condition uncertainty scenarios (scenarios B1-4). Variance from the first scenario arises only from demographic stochasticity (orange). Parameter, meteorological, and process uncertainty are added sequentially in the next three scenarios. The dotted lines on all the plots are the 95% credible intervals of the data estimated from tree rings.

Variance partitioning showed that the covariance between the initial condition uncertainty and the other types of uncertainties was the dominant variance contributor over time (hashed areas in Figure 8). All model scenarios that were run with model spin-up had much larger uncertainty than with data constrained initial conditions (Figure 6, column 1 versus column 2). In addition, initial conditions had long lasting affects on the magnitude of the total forecast variance (Figure 8). Notably, covariance between initial condition uncertainty and parameter, meteorological driver, and process variance decreased significantly over time while the interaction between initial conditions and demographic stochasticity slightly increased. Overall comparing scenarios A1-4 to scenarios B1-4 showed that this one time constraint was able to limit the total variance for 50+ years. The exponential decay constant of the effect of the initial conditions on total biomass

variance was .08/year, meaning that the half life of the effects of initial condition constraint is 4.25 years. However, after 50 years the total forecast variance of the spin up initial conditions was still 12.24% higher than the total forecast variance of the data constrained initial conditions. Process uncertainty decreased in its relative contribution to total variance over time whereas meteorological uncertainty increased over time (Figure 8). The increase in uncertainty contribution from meteorological uncertainty was largely due to its covariance with initial conditions.

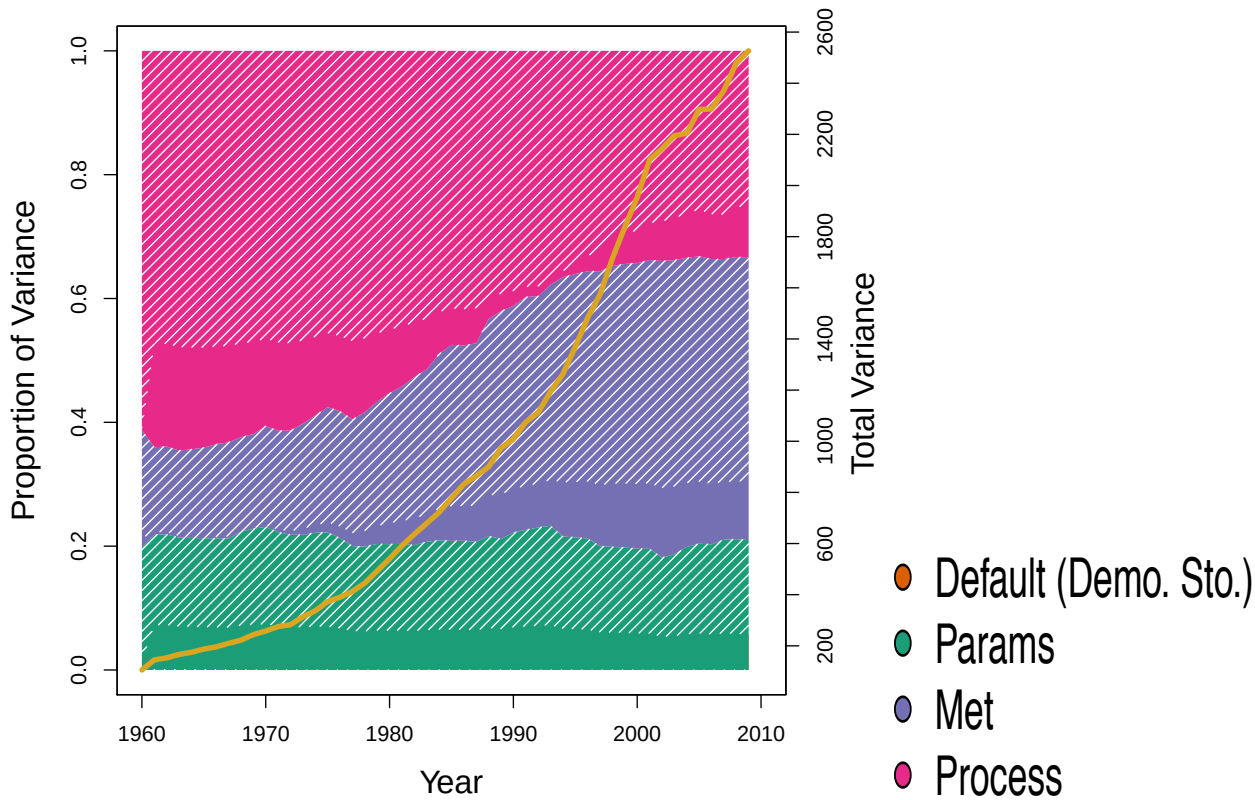

Figure 8: The relative contribution of each type of variance to total aboveground biomass variance. The hashed areas are the relative variances that can be attributed to the covariance with initial conditions. For example, over time initial condition uncertainty covariance with meteorological uncertainty (purple) accounted for a larger proportion of total variance.

We did not assimilate soil carbon data, so we considered the soil carbon uncertainty separately from aboveground biomass uncertainty. Similarly to the aboveground biomass variance partitioning, the data derived initial conditions did offer more constraint than spin up based initial conditions (Figure 9, left). In addition, process variance dominates by an order of magnitude, reflecting the lack of data constraint on this carbon pool. The covariance between initial conditions and process variance is an increasingly substantial

component over time (Figure 9, right).

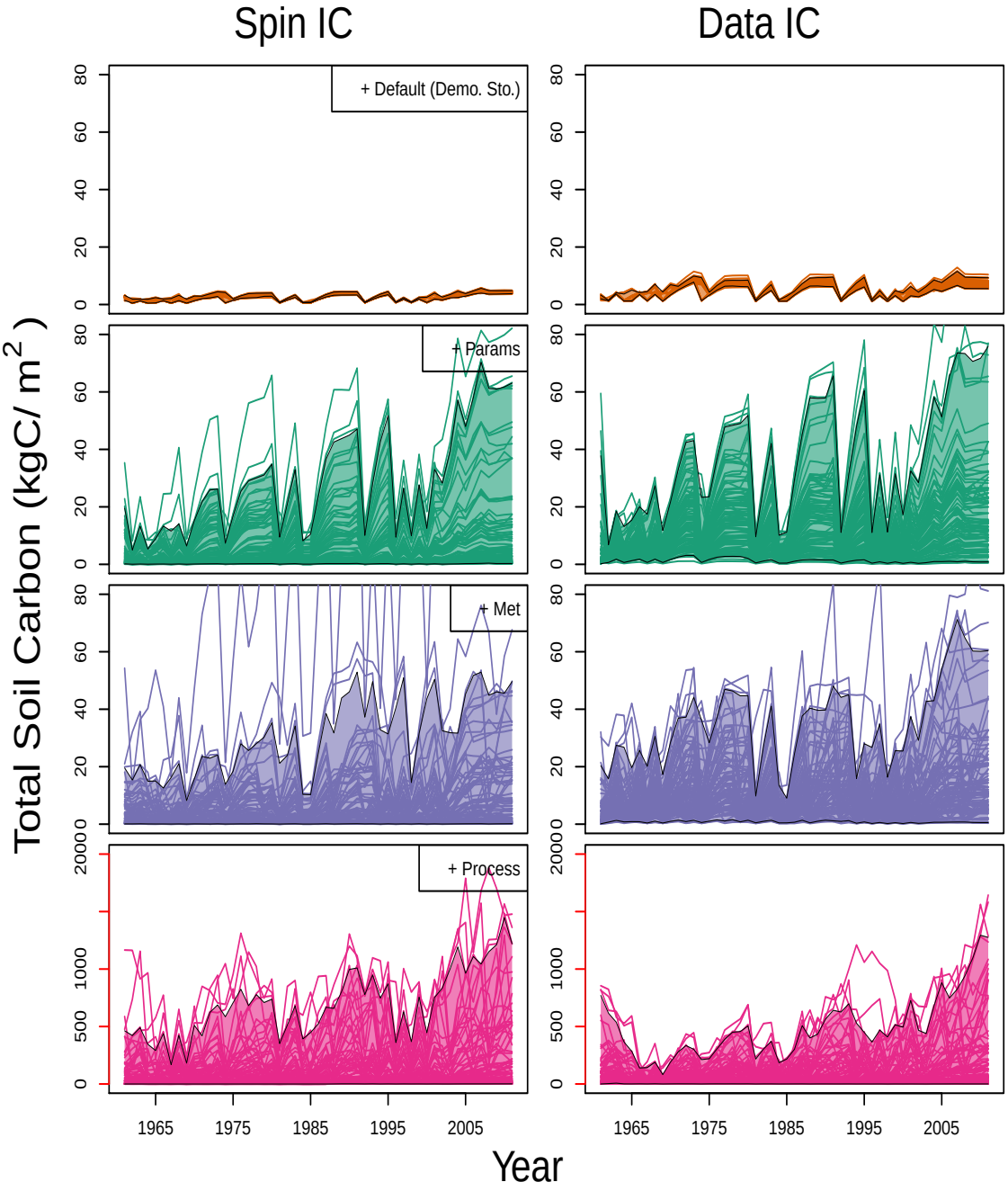

Figure 9: Individual model ensemble members overlaid with shaded 95% quantiles (outlined in black) of total soil carbon results from each uncertainty scenario using spin up as the model's initial conditions (left) and using data to constrain the model's initial conditions (right). Default was ran with initial condition uncertainty and internal model demographic stochasticity (first row). Next, parameter uncertainty was added (second row), followed by meteorological uncertainty (third row), and finally process error (fourth row).

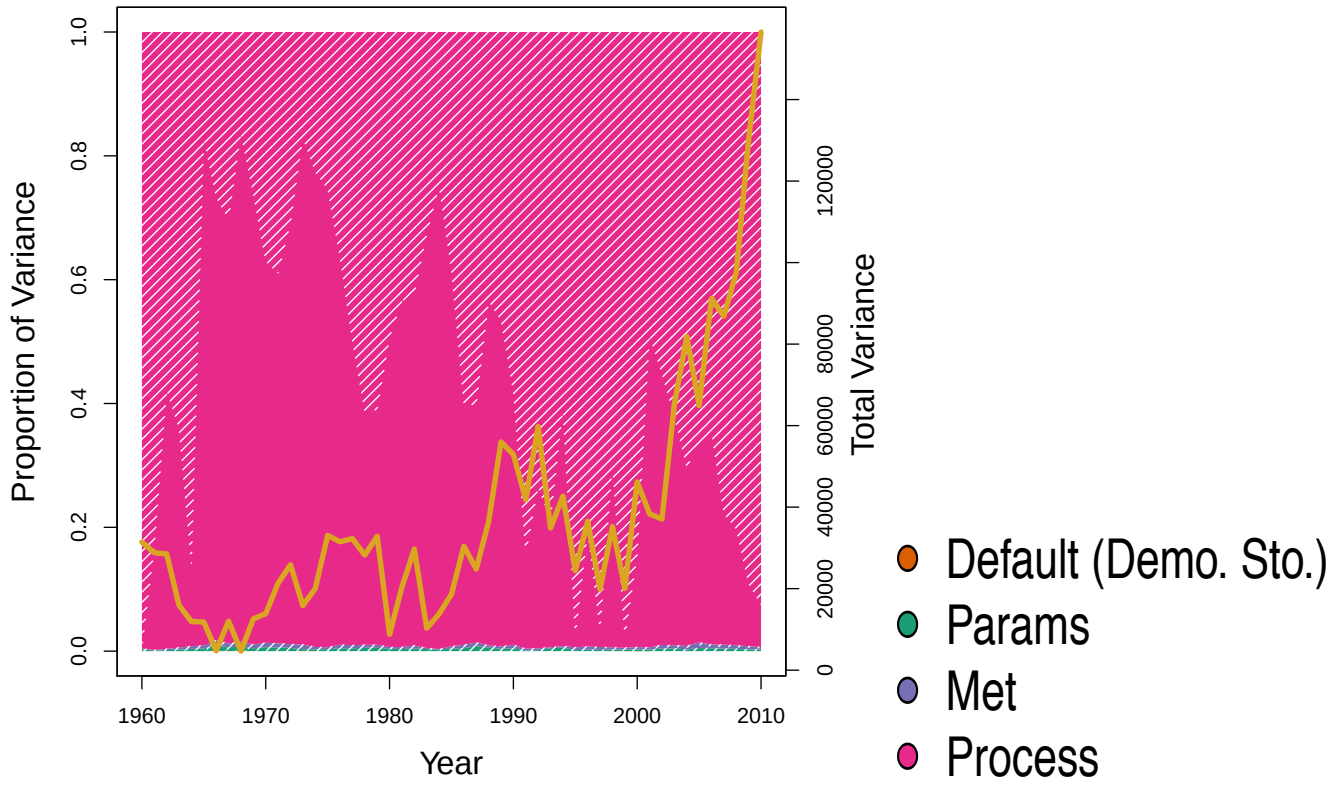

Figure 10: Relative contribution of each type of variance to total soil carbon variance. The grayed out areas are the amounts of variance that can be attributed to the covariance with initial conditions. Process (pink) uncertainties contributed a large amount of proportional variance to covariance with initial condition uncertainty.

4 Discussion

4.1 Partitioning variances in a forest gap model example

It has been demonstrated that incorporating uncertainty in predictive ecological models is important in several contexts (Clark et al. 2001; Dietze 2017b; Cressie et al. 2009), and forest community ecology is no exception. We found that incorporating uncertainty in initial conditions, environmental drivers, parameters, and processes led to decreased forecast precision but increased forecast accuracy. Our results indicate that relying on demographic stochasticity alone to capture the variability in ecological processes results in overconfident and inaccurate model hindcasts. This overconfidence from a forest gap model is concerning because in the vast majority (14/15) of forest gap model forecasts we studied, demographic stochasticity was the only source of uncertainty explicitly considered (Morin et al. 2014; Fischer et al. 2014, 2015, 2016;

Gutiérrez et al. 2016; Foster et al. 2017; Taylor et al. 2017; Chauvet et al. 2017; Rödig et al. 2017b,a; Sun et al. 2018; Boulanger et al. 2018; Rödig et al. 2018). Predictions using stochastic forecast gap models could be misleading scientists, managers, and policy makers because the model projections appear precise, while also appearing to account for uncertainty, but are only accounting for a tiny fraction (0.09%) of uncertainty in the projection in our case study.

Our analysis suggests that focusing efforts on data constrained initialization will be the most successful approach for improving forecast accuracy in forest gap models (68% reduction in total forecast variance from data constraints), even on multidecadal timescales. Typically, terrestrial ecosystem models are spun up to equilibrium (Sitch et al. 2003; Thornton and Rosenbloom 2005) before running forecasts or hindcasts. Model equilibrium assumptions are often relied upon because slow variables like soil carbon are difficult to constrain even with long-term data (Todd-Brown et al. 2013; Vereecken et al. 2016). We did not constrain soil carbon with data derived initial conditions in our analysis, and this led to high uncertainty in the total soil carbon pool, which we argue is a more honest representation of our uncertainty than assuming a tightly-constrained equilibrium state. Our analysis shows that initial condition uncertainty persists over long periods in forest gap models and the overall forecast uncertainty can be reduced significantly both by using data constrained initial conditions and by using state data assimilation to iteratively update state variables as new data becomes available. Our work agrees with Alexander et al. (2017) and Ge et al. (2018) showing that model spin up, and underlying equilibrium assumptions, could lead to very large, persistent uncertainties, especially in forested ecosystems where forest successional trajectories, landscape-level patch mosaic dynamics, and slow accumulation of soil carbon operate at centennial to millennial time scales (Watt, 1947; Jenny, 1941). Furthermore, our work provides evidence that these long lasting phenomena may be more important than Earth systems models have assumed (Bonan et al. 2018; Cox and Stephenson 2007).

Our estimate of process variance in LINKAGES over the data assimilation time period suggests that there are errors in modeled species mortality and recruitment, especially in red maple, that led to large process variances over 50 years. As discussed previously, plant demography, in general, is not well constrained over decadal to centennial time periods and may underpin global biomass changes as climate change shifts species ranges (Morin et al. 2018). Previously, mortality has been strongly linked to tree size (Lines et al. 2010; Dietze and Moorcroft 2011), but until recent advances with remote sensing, we lacked global scale tree mortality datasets (Smith et al. 2014). Vegetation recruitment is also difficult to represent in terrestrial models because dispersal rates are not well estimated and establishment in the understory cannot be seen by remote sensing, except following severe disturbance (Ibanez et al. 2008). Calibration efforts are underway to constrain demographic rates in dynamic vegetation models (Fischer et al. 2019; Fisher et al. 2019; Fer et al. 2018; Reichstein et al. 2019; Raczka et al. 2018). These efforts, along with the estimation of process variance,

will help assess the mathematical representations of demographic processes themselves by comparing process variance for different model types (Bugmann et al. 2019; Cailleret et al. 2020).

Typically, forest gap models are tuned to fixed parameter values in order to match independent data, and if parameter variance is included, it is not often separated from other types of uncertainty (Wramneby et al. 2008). Overemphasis on local parameter tuning may lead to overconfidence in predictions and will decrease the ability of a model to be generalizable across new sites. Model calibration and inclusion of parameter variance via ensemble methods are rapidly becoming much more common practice in ecosystem modeling (Fischer et al. 2019; Fisher et al. 2019; Fer et al. 2018; Reichstein et al. 2019; Raczka et al. 2018). Here, we informed our parameter distributions with an independent meta-analysis, but did not perform an additional calibration, and this decision may have increased our estimated process variance. On the other hand, the overall contribution of parameter uncertainty was relatively modest (18%) suggesting parameter variance is not a dominant source of uncertainty in our analysis.

We found that meteorological uncertainty was increasingly important over decadal time scale hindcasts, agreeing with work that shows that future climate scenarios are important to construct carefully (Feddema et al. 2005), in conjunction with data constrained initial conditions. Previous work has suggested that meteorological uncertainty increases over time in comparison to parameter uncertainty (Lovenduski and Bonan 2017; Bonan et al. 2018), but our analysis adds to this point by showing that the covariance between initial condition uncertainty and meteorological uncertainty may be contributing to the long-term increase observed by more complex forest demographic models (Raczka et al., 2018).

4.2 Future directions for improving terrestrial model predictions

Long-term data is imperative for improving forecast accuracy of the long-term carbon cycle. Here, long-term data allowed us to partition which aspects of variance are most important to constrain: demographic stochasticity, parameter, meteorological, or process uncertainties. In our analysis, we use a simple model built for understanding forest succession and showed that initial condition and process variance dominated at a decadal time scale. To reduce these uncertainties, future efforts should focus on 1) reducing initial condition uncertainty in terrestrial ecosystem models via data-driven initialization and data assimilation 2) further partitioning process uncertainty into reducible and irreducible components (e.g. model structure versus inherent stochasticity), and 3) determining whether these results are consistent across different terrestrial ecosystem models, biomes, and spatial and temporal scales. Below we expand on these three points then move to discussing broader implications for global change modeling.

Large scale data are becoming more available for terrestrial ecosystem model initialization, with ad-

vances in airborne and remote sensing measurements being particularly transformative. Not only can optical measurements be used to map canopy properties like leaf area index (LAI), but recent technological advancements in lidar, radar, and microwave remote sensing have improved our ability to map structural plant characteristics, like volume and canopy height, that are more directly related to terrestrial carbon pools, like total aboveground biomass (Goetz et al. 2009; Le Toan et al. 2011; Chave et al. 2019; Schepaschenko et al. 2019; Smith et al. 2020) as well as abiotic initial conditions, such as soil moisture (Entekhabi et al., 2010). In addition, hyperspectral remote sensing can provide us with the ability to map Plant Functional Type (PFTs) distribution globally (Shiklomanov et al., 2019). The Ecosystem Demography (ED) modeling team has demonstrated the effectiveness of remotely sensed Light Detection and Ranging (LiDAR) data for constraining initial conditions and decreasing near term forecast uncertainty (Hurtt et al. 2004; Antonarakis et al. 2014), a capacity that is now becoming applicable anywhere via the the Global Ecosystem Dynamics Investigation (GEDI) global lidar data product (Dubayah et al., 2020). These new measurements will provide terrestrial ecosystem models with significantly better data derived initial condition constraints than current spin up approaches (Schimel et al. 2015) and will greatly reduce uncertainty in both near-term and long-term forecasts of forested ecosystems.

While data on aboveground terrestrial carbon pools are becoming more available, it remains difficult to constrain below ground carbon pools with data because soil carbon is typically measured at the point level and interpolated over larger spatial scales (Vereecken et al. 2016). In addition, even though large scale datasets for below-ground carbon do exist (Todd-Brown et al. 2013), most large-scale soil carbon maps are ambiguous about what specific time point they represent and more modeling research is needed to determine the near-term and long-term prediction effects of constraining below-ground carbon with data derived initial conditions versus spin up initial conditions.

Model inter-comparisons studies have often found that process uncertainty is important for understanding model predictive ability (Joos et al. 2001; Knorr and Heimann 2001; Smith et al. 2001; Huntingford et al. 2008; Bugmann et al. 2019), but the approach usually taken (i.e., multiple models run deterministically under their default parameters and spin-up initial conditions) confounds multiple sources of uncertainty (i.e., process, parameter, initial conditions). At the same time, relying on multi-model spread as a measure of process error does not propagate residual process error or provide an estimate of the process variance relative to total forecast uncertainty. Multi-model ensembles also face challenges of independence because the set of models considered are never a random sample of the set of possible model structures (Sanderson et al. 2015; Tebaldi and Knutti 2007). By contrast, when long-term data was assimilated into our forest gap model, we were able to formally quantify and propagate the dynamic process uncertainty for the first time. This allowed us to partition process variance and separate its influence from other sources of uncertainty.

We found that even though our estimates of process variance at any given time step were small, on average process variance was much more influential on forecast uncertainty than environmental drivers or parameter uncertainty because the uncertainty compounds over time. This assessment suggests that to move forward with realistic assessments of forecast accuracy, we need to begin estimating and including process uncertainty in process-based models. Process variance can be conflated with parameter error if the model parameters are not calibrated because incorrect parameters will allow the modeled processes to drift from the data even if the model processes themselves are correct. We find that constraining parameter distributions with independent data is crucial for model improvement (Fer et al. 2018) and that de-convolving parameter uncertainty from other types of uncertainty allows us to pinpoint priority areas for model development. It is critical to apply variance partitioning approaches to more models of varying complexity to assess when and where additional complexity is statistically justified, and where the addition of unconstrained parameters causes the parameter uncertainty to increase more than process variance decreases. Understanding the amount of process variance that is reducible due to model structure, versus irreducible due to inherent stochasticity, would allow ecologists to quantify the amount of model development required to most accurately represent their system.

Comparing variance partitioning analyses across different terrestrial ecosystem models, biomes, and spatial and temporal scales is an important next step to understanding the generality of our findings. Using our process variance estimation to compare to estimations from other models with different representations of forest demographics would be a useful next step for understanding the variability across models and potentially partitioning process error into subcomponents (e.g., model structure, inherent stochasticity). Furthermore, estimating process variance across different ecosystems and model types using consistent analyses would allow us to quantify where ecosystem processes are and are not aligned with observational data. Fortunately, our state data assimilation algorithm is implemented within the Predictive Ecosystem Analyzer (PEcAn), a generalized model-data informatics system which allows for multiple models to be run and constrained with identical methodology and datasets. By using similar methodologies with comparable outputs we will be more able to tease apart the uncertainties underlying predictability of global terrestrial ecosystems.

4.3 Implications for global change biology

Beyond terrestrial ecosystems, most ecological forecasts are made without the inclusion of key uncertainties, with many made purely deterministically, leaving out uncertainty quantification all together (Cressie et al., 2009). This common practice creates projections that may be precise but are often inaccurate. Similarly, many ecological fields focus on specific aspects of uncertainty without considering a full suite of possibili-

ties. In particular, our finding that demographic stochastic is not the dominant uncertainty on forest gap models likely extends more broadly, suggesting that the current reliance on stochastic models may be misleading ecologists about the dominant drivers of uncertainty. Similarly, many ecological projections have focused on uncertainty in parameters and meteorological drivers (Kremer, 1983; Eberhardt, 1987; Regan et al., 2002; Grimm et al., 2005; Zwart et al., 2019). While it's clear that these uncertainties do contribute to ecological modeling in general, it remains unclear what the relative contributions of parameter and meteorological uncertainty are to total forecast uncertainty across different spatial and temporal scales. For example, conventional wisdom suggests that initial condition uncertainties are likely to dominate on very short timescales, and climate scenario uncertainty is likely to dominate on very long timescales (Cox and Stephenson 2007), but when the crossover occurs could vary enormously across systems, as could the impacts of other uncertainties.

Our analysis showed that initial conditions and process variance were dominant sources of uncertainty, and interestingly, these uncertainties are largely overlooked across many ecological process-based models. Process-based models frequently include the idea of ecological memory, or cumulative effects, which has been shown to be a dominant force in determining the trajectory of many types of ecological systems (Peterson, 2002; Ogle et al., 2015; Hughes et al., 2019). Because of the effects of ecological memory, we hypothesize that constraining initial conditions with available datasets will allow for the largest and quickest increases in predictive accuracy, and decreases in forecast uncertainty, across ecological process-based models. Furthermore, complex ecological systems often feature high dimensional interactions between state variables. This leads to process-based models that are highly and increasingly complex. It is often unclear if increased model complexity is leading to increased predictive accuracy (Green et al., 2005; Hooten and Hobbs, 2015). Estimating process variance, and determining the amount of reducible versus irreducible process variance, would illuminate the need for altering modelled processes or changing model complexity. Through the development of new data assimilation approaches, our estimation moves beyond typically calculated residual and validation errors, providing an estimate of process variance that is dynamic (time-point to time-point) and quantifies the uncertainty remaining after accounting for all the other uncertainties discussed above, including observation error. Furthermore, we highlight the critical importance of propagating process error into ecological forecasts, which heretofore has generally been absent from process modeling approaches.

In conclusion, improving predictions of ecosystems properties not only leads to enhancements for decision makers and stakeholders but also more efficient progress in advancing basic research and theory. Here, we demonstrate the power uncertainty quantification has in ecology to reveal which long-standing modeling assumptions (spin-up initial conditions, stochastic models are sufficient to capture uncertainties, process error is negligible) are not upheld by data and what steps can be taken to immediately increase forecast

accuracy in the terrestrial carbon cycle. These lessons are not unique to terrestrial ecology. Demographic stochasticity, parameter, meteorological, and process uncertainties are quantities that are measured across ecology and can be used to quantitatively move toward better and more useful ecological predictions.

Acknowledgements

This material is based upon work supported by the National Science Foundation MacroSystems Biology under grant no. DEB-1241874, 1241891, 1458021. The authors thank the PalEON and PEcAn teams for support in early development of this project. We also thank Harvard Forest scientists Neil Pederson and Audrey Barker Plotkin for collecting and archiving the field data behind the aboveground biomass estimates.

Author Contributions

AR, MD, and JM designed project; AR and MD developed the data assimilation algorithm; AR analyzed data with advice from MD and JM; AR, JM, and MD wrote paper with further text contributions from all authors in the Supplementary Materials. Specifically, AD created and fit the tree ring model to create the species level biomass estimates, CR downscaled the climate drivers used to drive the model in this analysis, and JT fit the model that calculated the climate driver weights. All data and code used for this analysis is available in the manuscript supplementary materials or publicly on GitHub.

References

Alexander, P., R. Prestele, P. H. Verburg, A. Arneth, C. Baranzelli, F. Batista e Silva, C. Brown, A. Butler, K. Calvin, N. Dendoncker, et al., 2017. Assessing uncertainties in land cover projections. *Global change biology* **23**:767–781.

Anderson, J., T. Hoar, K. Raeder, H. Liu, N. Collins, R. Torn, and A. Avellano, 2009. The data assimilation research testbed: A community facility. *Bulletin of the American Meteorological Society* **90**:1283–1296.

Anderson, J. L., 2001. An ensemble adjustment Kalman filter for data assimilation. *Monthly weather review* **129**:2884–2903.

Antonarakis, A., J. Munger, and P. Moorcroft, 2014. Imaging spectroscopy-and lidar-derived estimates of canopy composition and structure to improve predictions of forest carbon fluxes and ecosystem dynamics. *Geophysical Research Letters* **41**:2535–2542.

Bonan, G., 2015. Ecological climatology: concepts and applications. Cambridge University Press.

Bonan, G. B., D. L. Lombardozzi, W. R. Wieder, K. W. Oleson, D. M. Lawrence, F. M. Hoffman, and N. Collier, 2018. Model structure and climate data uncertainty in historical simulations of the terrestrial carbon cycle (1850–2014). *Global Biogeochemical Cycles* .

Botkin, D. B., J. F. Janak, and J. R. Wallis, 1972. Some ecological consequences of a computer model of forest growth. *The Journal of Ecology* pages 849–872.

Boulanger, Y., A. R. Taylor, D. T. Price, D. Cyr, and G. Sainte-Marie, 2018. Stand-level drivers most important in determining boreal forest response to climate change. *Journal of Ecology* **106**:977–990.

Bugmann, H., 2001. A review of forest gap models. *Climatic Change* **51**:259–305.

Bugmann, H., R. Seidl, F. Hartig, F. Bohn, J. Bruna, M. Cailleret, L. Francois, J. Heinke, A. Henrot, T. Hickler, et al., 2019. Tree mortality submodels drive simulated long-term forest dynamics: assessing 15 models from the stand to global scale. *Ecosphere* **10**:e02616.

Bugmann, H. K., X. Yan, M. T. Sykes, P. Martin, M. Lindner, P. V. Desanker, and S. G. Cumming, 1996. A comparison of forest gap models: model structure and behaviour. *Climatic Change* **34**:289–313.

Cailleret, M., N. Bircher, F. Hartig, L. Hülsmann, and H. Bugmann, 2020. Bayesian calibration of a growth-dependent tree mortality model to simulate the dynamics of european temperate forests. *Ecological Applications* **30**:e02021.

Catovsky S, B. F., 2000. Linking community dynamics and ecosystem function at harvard forest 1996-2000. *Harvard Forest Data Archive: HF035* .

Chauvet, M., G. Kunstler, J. Roy, and X. Morin, 2017. Using a forest dynamics model to link community assembly processes and traits structure. *Functional Ecology* **31**:1452–1461.

Chave, J., S. J. Davies, O. L. Phillips, S. L. Lewis, P. Sist, D. Schepaschenko, J. Armston, T. R. Baker, D. Coomes, M. Disney, et al., 2019. Ground data are essential for biomass remote sensing missions. *Surveys in Geophysics* **40**:863–880.

Clark, J. S. and O. N. Bjørnstad, 2004. Population time series: process variability, observation errors, missing values, lags, and hidden states. *Ecology* **85**:3140–3150.

Clark, J. S., S. R. Carpenter, M. Barber, S. Collins, A. Dobson, J. A. Foley, D. M. Lodge, M. Pascual, R. Pielke, W. Pizer, et al., 2001. Ecological forecasts: an emerging imperative. *Science* **293**:657–660.

Cook, E. R., R. Seager, R. R. Heim Jr, R. S. Vose, C. Herweijer, and C. Woodhouse, 2010. Megadroughts in North America: Placing IPCC projections of hydroclimatic change in a long-term palaeoclimate context. *Journal of Quaternary Science* **25**:48–61.

Cox, P. and D. Stephenson, 2007. A changing climate for prediction. *Science* **317**:207–208.

Cressie, N., C. A. Calder, J. S. Clark, J. M. V. Hoef, and C. K. Wikle, 2009. Accounting for uncertainty in ecological analysis: the strengths and limitations of hierarchical statistical modeling. *Ecological Applications* **19**:553–570.

de Valpine, P., D. Turek, C. J. Paciorek, C. Anderson-Bergman, D. T. Lang, and R. Bodik, 2017. Programming with models: writing statistical algorithms for general model structures with NIMBLE. *Journal of Computational and Graphical Statistics* **26**:403–413.

Dietze, M. C., 2017a. Ecological forecasting. Princeton University Press.

Dietze, M. C., 2017b. Prediction in ecology: a first-principles framework. *Ecological Applications* **27**:2048–2060.

Dietze, M. C., D. S. LeBauer, and R. Kooper, 2013. On improving the communication between models and data. *Plant, Cell & Environment* **36**:1575–1585.

Dietze, M. C. and P. R. Moorcroft, 2011. Tree mortality in the eastern and central u nited s tates: patterns and drivers. *Global Change Biology* **17**:3312–3326.

Dietze, M. C., M. S. Wolosin, and J. S. Clark, 2008. Capturing diversity and interspecific variability in allometries: a hierarchical approach. *Forest Ecology and Management* **256**:1939–1948.

Dubayah, R., J. B. Blair, S. Goetz, L. Fatoyinbo, M. Hansen, S. Healey, M. Hofton, G. Hurtt, J. Kellner, S. Luthcke, et al., 2020. The global ecosystem dynamics investigation: High-resolution laser ranging of the Earthâs forests and topography. *Science of Remote Sensing* **1**:100002.

Dye, A., A. Barker Plotkin, D. Bishop, N. Pederson, B. Poulter, and A. Hessl, 2016. Comparing tree-ring and permanent plot estimates of aboveground net primary production in three eastern US forests. *Ecosphere* **7**.

Eberhardt, L., 1987. Population projections from simple models. *Journal of Applied Ecology* pages 103–118.

Entekhabi, D., E. G. Njoku, P. E. O'Neill, K. H. Kellogg, W. T. Crow, W. N. Edelstein, J. K. Entin, S. D. Goodman, T. J. Jackson, J. Johnson, et al., 2010. The soil moisture active passive (SMAP) mission. *Proceedings of the IEEE* **98**:704–716.

Evensen, G., 2009. The ensemble Kalman filter for combined state and parameter estimation. *IEEE Control Systems Magazine* **29**:83–104.

Feddema, J. J., K. W. Oleson, G. B. Bonan, L. O. Mearns, L. E. Buja, G. A. Meehl, and W. M. Washington, 2005. The importance of land-cover change in simulating future climates. *Science* **310**:1674–1678.

Fer, I., R. Kelly, P. R. Moorcroft, A. D. Richardson, E. M. Cowdery, and M. C. Dietze, 2018. Linking big models to big data: efficient ecosystem model calibration through Bayesian model emulation. *Biogeosciences* **15**:5801–5830.

Fischer, F. J., I. Maréchaux, and J. Chave, 2019. Improving plant allometry by fusing forest models and remote sensing. *New Phytologist* **223**:1159–1165.

Fischer, R., A. Armstrong, H. H. Shugart, and A. Huth, 2014. Simulating the impacts of reduced rainfall on carbon stocks and net ecosystem exchange in a tropical forest. *Environmental Modelling & Software* **52**:200–206.

Fischer, R., F. Bohn, M. D. de Paula, C. Dislich, J. Groeneveld, A. G. Gutiérrez, M. Kazmierczak, N. Knapp, S. Lehmann, S. Paulick, et al., 2016. Lessons learned from applying a forest gap model to understand ecosystem and carbon dynamics of complex tropical forests. *Ecological Modelling* **326**:124–133.

Fischer, R., A. Ensslin, G. Rutten, M. Fischer, D. S. Costa, M. Kleyer, A. Hemp, S. Paulick, and A. Huth, 2015. Simulating carbon stocks and fluxes of an African tropical montane forest with an individual-based forest model. *PLoS One* **10**:e0123300.

Fisher, R. A., C. D. Koven, W. R. Anderegg, B. O. Christoffersen, M. C. Dietze, C. E. Farrior, J. A. Holm, G. C. Hurtt, R. G. Knox, P. J. Lawrence, et al., 2018. Vegetation demographics in Earth system models: A review of progress and priorities. *Global Change Biology* **24**:35–54.

Fisher, R. A., W. R. Wieder, B. M. Sanderson, C. D. Koven, K. W. Oleson, C. Xu, J. B. Fisher, M. Shi, A. P. Walker, and D. M. Lawrence, 2019. Parametric controls on vegetation responses to biogeochemical forcing in the CLM5. *Journal of Advances in Modeling Earth Systems* **11**:2879–2895.

Foster, A. C., J. K. Shuman, H. H. Shugart, K. A. Dwire, P. J. Fornwalt, J. Sibold, and J. Negron, 2017. Validation and application of a forest gap model to the southern Rocky Mountains. *Ecological Modelling* **351**:109–128.

Foster, D. R. and J. D. Aber, 2006. Forests in time: the environmental consequences of 1,000 years of change in New England. Yale University Press.

Friedlingstein, P., M. Meinshausen, V. K. Arora, C. D. Jones, A. Anav, S. K. Liddicoat, and R. Knutti, 2014. Uncertainties in cmip5 climate projections due to carbon cycle feedbacks. *Journal of Climate* **27**:511–526.

Friend, A. D., W. Lucht, T. T. Rademacher, R. Keribin, R. Betts, P. Cadule, P. Ciais, D. B. Clark, R. Dankers, P. D. Falloon, et al., 2014. Carbon residence time dominates uncertainty in terrestrial vegetation responses to future climate and atmospheric CO2. *Proceedings of the National Academy of Sciences* **111**:3280–3285.

Ge, R., H. He, X. Ren, L. Zhang, G. Yu, T. L. Smallman, T. Zhou, S.-Y. Yu, Y. Luo, Z. Xie, et al., 2018. Underestimated ecosystem carbon turnover time and sequestration under the steady state assumption: A perspective from long-term data assimilation. *Global Change Biology* .

Gelman, A., D. B. Rubin, et al., 1992. Inference from iterative simulation using multiple sequences. *Statistical Science* **7**:457–472.

Goetz, S. J., A. Baccini, N. T. Laporte, T. Johns, W. Walker, J. Kellndorfer, R. A. Houghton, and M. Sun, 2009. Mapping and monitoring carbon stocks with satellite observations: a comparison of methods. *Carbon Balance and Management* **4**:2.

Goodman, D., 1987. Consideration of stochastic demography in the design and management of biological reserves. *Natural Resource Modeling* **1**:205–234.

Green, J. L., A. Hastings, P. Arzberger, F. J. Ayala, K. L. Cottingham, K. Cuddington, F. Davis, J. A. Dunne, M.-J. Fortin, L. Gerber, et al., 2005. Complexity in ecology and conservation: mathematical, statistical, and computational challenges. *BioScience* **55**:501–510.

Grimm, V., E. Revilla, U. Berger, F. Jeltsch, W. M. Mooij, S. F. Railsback, H.-H. Thulke, J. Weiner, T. Wiegand, and D. L. DeAngelis, 2005. Pattern-oriented modeling of agent-based complex systems: lessons from ecology. *science* **310**:987–991.

Gutiérrez, A. G., R. S. Snell, and H. Bugmann, 2016. Using a dynamic forest model to predict tree species distributions. *Global Ecology and Biogeography* **25**:347–358.

Hall, D. B., 2000. Zero-inflated Poisson and binomial regression with random effects: a case study. *Biometrics* **56**:1030–1039.

Hawkins, E. and R. Sutton, 2009. The potential to narrow uncertainty in regional climate predictions. *Bulletin of the American Meteorological Society* **90**:1095–1108.

Hewitt, A. J., B. B. Booth, C. D. Jones, E. S. Robertson, A. J. Wiltshire, P. G. Sansom, D. B. Stephenson, and S. Yip, 2016. Sources of uncertainty in future projections of the carbon cycle. *Journal of Climate* **29**:7203–7213.

Hooten, M. B. and N. T. Hobbs, 2015. A guide to Bayesian model selection for ecologists. *Ecological Monographs* **85**:3–28.

Hughes, T. P., J. T. Kerry, S. R. Connolly, A. H. Baird, C. M. Eakin, S. F. Heron, A. S. Hoey, M. O. Hoogenboom, M. Jacobson, G. Liu, et al., 2019. Ecological memory modifies the cumulative impact of recurrent climate extremes. *Nature Climate Change* **9**:40–43.

Hui, D., Y. Luo, and G. Katul, 2003. Partitioning interannual variability in net ecosystem exchange between climatic variability and functional change. *Tree Physiology* **23**:433–442.

Huntingford, C., R. A. Fisher, L. Mercado, B. B. Booth, S. Sitch, P. P. Harris, P. M. Cox, C. D. Jones, R. A. Betts, Y. Malhi, et al., 2008. Towards quantifying uncertainty in predictions of Amazon 'dieback'. *Philosophical Transactions of the Royal Society of London B: Biological Sciences* **363**:1857–1864.

Hurtt, G. C., R. Dubayah, J. Drake, P. R. Moorcroft, S. W. Pacala, J. B. Blair, and M. G. Fearon, 2004. Beyond potential vegetation: Combining lidar data and a height-structured model for carbon studies. *Ecological Applications* **14**:873–883.

Hyndman, R. J. and A. B. Koehler, 2006. Another look at measures of forecast accuracy. *International Journal of Forecasting* **22**:679–688.

Ibanez, I., J. S. Clark, and M. C. Dietze, 2008. Evaluating the sources of potential migrant species: implications under climate change. *Ecological Applications* **18**:1664–1678.

Jenny, H., 1941. Factors of soil formation. 281 pp. *New York* .

Joos, F., I. C. Prentice, S. Sitch, R. Meyer, G. Hooss, G.-K. Plattner, S. Gerber, and K. Hasselmann, 2001. Global warming feedbacks on terrestrial carbon uptake under the intergovernmental panel on climate change (IPCC) emission scenarios. *Global Biogeochemical Cycles* **15**:891–907.

Kalman, R. E., 1960. A new approach to linear filtering and prediction problems. *Journal of Basic Engineering* **82**:35–45.

Keenan, T., I. Baker, A. Barr, P. Ciais, K. Davis, M. Dietze, D. Dragoni, C. M. Gough, R. Grant, D. Hollinger, et al., 2012. Terrestrial biosphere model performance for inter-annual variability of land-atmosphere CO2 exchange. *Global Change Biology* **18**:1971–1987.

Knorr, W. and M. Heimann, 2001. Uncertainties in global terrestrial biosphere modeling, part ii: Global constraints for a process-based vegetation model. *Global Biogeochemical Cycles* **15**:227–246.

Kremer, J. N., 1983. Ecological implications of parameter uncertainty in stochastic simulation. *Ecological Modelling* **18**:187–207.

Lande, R., 1993. Risks of population extinction from demographic and environmental stochasticity and random catastrophes. *The American Naturalist* **142**:911–927.

Le Toan, T., S. Quegan, M. Davidson, H. Balzter, P. Paillou, K. Papathanassiou, S. Plummer, F. Rocca, S. Saatchi, H. Shugart, et al., 2011. The biomass mission: Mapping global forest biomass to better understand the terrestrial carbon cycle. *Remote Sensing of Environment* **115**:2850–2860.

LeBauer, D., R. Kooper, P. Mulrooney, S. Rohde, D. Wang, S. P. Long, and M. C. Dietze, 2018. Betydb: a yield, trait, and ecosystem service database applied to second-generation bioenergy feedstock production. *GCB Bioenergy* **10**:61–71.

LeBauer, D. S., D. Wang, K. T. Richter, C. C. Davidson, and M. C. Dietze, 2013. Facilitating feedbacks between field measurements and ecosystem models. *Ecological Monographs* **83**:133–154.

Lindner, M., R. Sievänen, and H. Pretzsch, 1997. Improving the simulation of stand structure in a forest gap model. *Forest Ecology and Management* **95**:183–195.

Lines, E. R., D. A. Coomes, and D. W. Purves, 2010. Influences of forest structure, climate and species composition on tree mortality across the eastern US. *PLoS One* **5**:e13212.

Lorenz, E. N., 1963. Deterministic nonperiodic flow. *Journal of the Atmospheric Sciences* **20**:130–141.

Lovenduski, N. S. and G. B. Bonan, 2017. Reducing uncertainty in projections of terrestrial carbon uptake. *Environmental Research Letters* **12**:044020.

Luo, Y., T. F. Keenan, and M. Smith, 2015. Predictability of the terrestrial carbon cycle. *Global Change Biology* **21**:1737–1751.

MacBean, N., F. Maignan, P. Peylin, C. Bacour, F.-M. Bréon, and P. Ciais, 2015. Using satellite data to improve the leaf phenology of a global terrestrial biosphere model. *Biogeosciences* **12**:7185–7208.

Mann, M. E., Z. Zhang, S. Rutherford, R. S. Bradley, M. K. Hughes, D. Shindell, C. Ammann, G. Faluvegi, and F. Ni, 2009. Global signatures and dynamical origins of the little ice age and medieval climate anomaly. *Science* **326**:1256–1260.

Martin, T. G., B. A. Wintle, J. R. Rhodes, P. M. Kuhnert, S. A. Field, S. J. Low-Choy, A. J. Tyre, and H. P. Possingham, 2005. Zero tolerance ecology: improving ecological inference by modelling the source of zero observations. *Ecology Letters* **8**:1235–1246.

Massoud, E. C., J. Huisman, E. Benincà, M. C. Dietze, W. Bouten, and J. A. Vrugt, 2018. Probing the limits of predictability: data assimilation of chaotic dynamics in complex food webs. *Ecology Letters* **21**:93–103.

Medlyn, B. E., S. Zaehle, M. G. De Kauwe, A. P. Walker, M. C. Dietze, P. J. Hanson, T. Hickler, A. K. Jain, Y. Luo, W. Parton, et al., 2015. Using ecosystem experiments to improve vegetation models. *Nature Climate Change* **5**:528.

Medvigy, D., S. C. Wofsy, J. W. Munger, and P. R. Moorcroft, 2010. Responses of terrestrial ecosystems and carbon budgets to current and future environmental variability. *Proceedings of the National Academy of Sciences* **107**:8275–8280.

Morin, X., L. Fahse, C. de Mazancourt, M. Scherer-Lorenzen, and H. Bugmann, 2014. Temporal stability in forest productivity increases with tree diversity due to asynchrony in species dynamics. *Ecology Letters* **17**:1526–1535.

Morin, X., L. Fahse, H. Jactel, M. Scherer-Lorenzen, R. García-Valdés, and H. Bugmann, 2018. Long-term response of forest productivity to climate change is mostly driven by change in tree species composition. *Scientific Reports* **8**:5627.

Munger W, W. S., 2018. Biomass inventories at harvard forest EMS tower since 1993. *Harvard Forest Data Archive: HF069* .

Neal, R. M., 2003. Slice sampling. *Annals of statistics* pages 705–741.

Nishina, K., A. Ito, P. Falloon, A. Friend, D. Beerling, P. Ciais, D. Clark, R. Kahana, E. Kato, W. Lucht, et al., 2015. Decomposing uncertainties in the future terrestrial carbon budget associated with emission scenarios, climate projections, and ecosystem simulations using the ISI-MIP results. *Earth System Dynamics* **6**:435–445.

Niu, S., Y. Luo, M. C. Dietze, T. F. Keenan, Z. Shi, J. Li, and F. S. C. III, 2014. The role of data assimilation in predictive ecology. *Ecosphere* **5**:1–16.

Ogle, K., J. J. Barber, G. A. Barron-Gafford, L. P. Bentley, J. M. Young, T. E. Huxman, M. E. Loik, and D. T. Tissue, 2015. Quantifying ecological memory in plant and ecosystem processes. *Ecology Letters* **18**:221–235.

Pacala, S. W., C. D. Canham, and J. Silander Jr, 1993. Forest models defined by field measurements: The design of a northeastern forest simulator. *Canadian Journal of Forest Research* **23**:1980–1988.

Padisak, J., 1992. Seasonal succession of phytoplankton in a large shallow lake (balaton, hungary)–a dynamic approach to ecological memory, its possible role and mechanisms. *Journal of Ecology* pages 217–230.

Papadakis, N., É. Mémin, A. Cuzol, and N. Gengembre, 2010. Data assimilation with the weighted ensemble Kalman filter. *Tellus A: Dynamic Meteorology and Oceanography* **62**:673–697.

Peterson, G. D., 2002. Contagious disturbance, ecological memory, and the emergence of landscape pattern. *Ecosystems* **5**:329–338.

Piao, S., S. Sitch, P. Ciais, P. Friedlingstein, P. Peylin, X. Wang, A. Ahlström, A. Anav, J. G. Canadell, N. Cong, et al., 2013. Evaluation of terrestrial carbon cycle models for their response to climate variability and to CO2 trends. *Global Change Biology* **19**:2117–2132.

Plummer, M., N. Best, K. Cowles, and K. Vines, 2006. Coda: convergence diagnosis and output analysis for MCMC. *R news* **6**:7–11.

Post, W. M. and J. Pastor, 1996. Linkages—an individual-based forest ecosystem model. *Climatic Change* **34**:253–261.

Poulter, B., F. Hattermann, E. Hawkins, S. Zaehle, S. Sitch, N. RESTREPO-COUPE, U. Heyder, and W. Cramer, 2010. Robust dynamics of Amazon dieback to climate change with perturbed ecosystem model parameters. *Global Change Biology* **16**:2476–2495.

Rabier, F., E. Klinker, P. Courtier, and A. Hollingsworth, 1996. Sensitivity of forecast errors to initial conditions. *Quarterly Journal of the Royal Meteorological Society* **122**:121–150.

Raczka, B., M. C. Dietze, S. P. Serbin, and K. J. Davis, 2018. What limits predictive certainty of long-term carbon uptake? *Journal of Geophysical Research: Biogeosciences* **123**:3570–3588.

Regan, H. M., M. Colyvan, and M. A. Burgman, 2002. A taxonomy and treatment of uncertainty for ecology and conservation biology. *Ecological applications* **12**:618–628.

Reichstein, M., G. Camps-Valls, B. Stevens, M. Jung, J. Denzler, N. Carvalhais, et al., 2019. Deep learning and process understanding for data-driven Earth system science. *Nature* **566**:195–204.

Roberts, G. O. and S. K. Sahu, 1997. Updating schemes, correlation structure, blocking and parameterization for the Gibbs sampler. *Journal of the Royal Statistical Society: Series B (Statistical Methodology)* **59**:291–317.

Rödig, E., M. Cuntz, J. Heinke, A. Rammig, and A. Huth, 2017a. Spatial heterogeneity of biomass and forest structure of the Amazon rain forest: Linking remote sensing, forest modelling and field inventory. *Global Ecology and Biogeography* **26**:1292–1302.

Rödig, E., M. Cuntz, A. Rammig, R. Fischer, F. Taubert, and A. Huth, 2018. The importance of forest structure for carbon fluxes of the Amazon rainforest. *Environmental Research Letters* **13**:054013.

Rödig, E., A. Huth, F. Bohn, C. Rebmann, and M. Cuntz, 2017b. Estimating the carbon fluxes of forests with an individual-based forest model. *Forest Ecosystems* **4**:4.

Rollinson, C. R., Y. Liu, A. Raiho, D. J. Moore, J. McLachlan, D. A. Bishop, A. Dye, J. H. Matthes, A. Hessl, T. Hickler, et al., 2017. Emergent climate and CO2 sensitivities of net primary productivity in ecosystem models do not agree with empirical data in temperate forests of eastern North America. *Global Change Biology* .

Sanderson, B. M., R. Knutti, and P. Caldwell, 2015. Addressing interdependency in a multimodel ensemble by interpolation of model properties. *Journal of Climate* **28**:5150–5170.

Scheller, R. M. and D. J. Mladenoff, 2004. A forest growth and biomass module for a landscape simulation model, LADIS: design, validation, and application. *Ecological Modelling* **180**:211–229.

Schepaschenko, D., J. Chave, O. L. Phillips, S. L. Lewis, S. J. Davies, M. Réjou-Méchain, P. Sist, K. Scipal, C. Perger, B. Hérault, et al., 2019. The forest observation system, building a global reference dataset for remote sensing of forest biomass. *Scientific Data* **6**:1–11.

Schimel, D., R. Pavlick, J. B. Fisher, G. P. Asner, S. Saatchi, P. Townsend, C. Miller, C. Frankenberg, K. Hibbard, and P. Cox, 2015. Observing terrestrial ecosystems and the carbon cycle from space. *Global Change Biology* **21**:1762–1776.

Shiklomanov, A. N., B. A. Bradley, K. M. Dahlin, A. M Fox, C. M. Gough, F. M. Hoffman, E. M Middleton, S. P. Serbin, L. Smallman, and W. K. Smith, 2019. Enhancing global change experiments through integration of remote-sensing techniques. *Frontiers in Ecology and the Environment* **17**:215–224.

Sitch, S., B. Smith, I. C. Prentice, A. Arneth, A. Bondeau, W. Cramer, J. Kaplan, S. Levis, W. Lucht, M. T. Sykes, et al., 2003. Evaluation of ecosystem dynamics, plant geography and terrestrial carbon cycling in the LPJ dynamic global vegetation model. *Global Change Biology* **9**:161–185.

Smith, A. M., C. A. Kolden, W. T. Tinkham, A. F. Talhelm, J. D. Marshall, A. T. Hudak, L. Boschetti, M. J. Falkowski, J. A. Greenberg, J. W. Anderson, et al., 2014. Remote sensing the vulnerability of vegetation in natural terrestrial ecosystems. *Remote Sensing of Environment* **154**:322–337.

Smith, B., I. C. Prentice, and M. T. Sykes, 2001. Representation of vegetation dynamics in the modelling of terrestrial ecosystems: comparing two contrasting approaches within European climate space. *Global Ecology and Biogeography* **10**:621–637.

Smith, W. K., A. M. Fox, N. MacBean, D. J. Moore, and N. C. Parazoo, 2020. Constraining estimates of terrestrial carbon uptake: new opportunities using long-term satellite observations and data assimilation. *New Phytologist* **225**:105–112.

Solomon, A. M., 1986. Transient response of forests to CO2 induced climate change: simulation modeling experiments in eastern North America. *Oecologia* **68**:567–579.

Solomon, A. M., H. R. Delcourt, D. C. West, and T. Blasing, 1980. Testing a simulation model for reconstruction of prehistoric forest-stand dynamics. *Quaternary Research* **14**:275–293.

Sullivan, F. B., M. J. Ducey, D. A. Orwig, B. Cook, and M. W. Palace, 2017. Comparison of lidar and allometry derived canopy height models in an eastern deciduous forest. *Forest Ecology and Management* **406**:83–94.

Sun, N., M. Wigmosta, T. Zhou, J. Lundquist, S. Dickerson-Lange, and N. Cristea, 2018. Evaluating the functionality and streamflow impacts of explicitly modelling forest–snow interactions and canopy gaps in a distributed hydrologic model. *Hydrological Processes* **32**:2128–2140.

Taylor, A. R., Y. Boulanger, D. T. Price, D. Cyr, E. McGarrigle, W. Rammer, and J. A. Kershaw Jr, 2017. Rapid 21st century climate change projected to shift composition and growth of Canada's Acadian Forest Region. *Forest ecology and management* **405**:284–294.

Team, N. D. et al., 2017. Nimble: An R package for programming with bugs models .

Tebaldi, C. and R. Knutti, 2007. The use of the multi-model ensemble in probabilistic climate projections. *Philosophical transactions of the royal society A: mathematical, physical and engineering sciences* **365**:2053–2075.

Thornton, P. E. and N. A. Rosenbloom, 2005. Ecosystem model spin-up: Estimating steady state conditions in a coupled terrestrial carbon and nitrogen cycle model. *Ecological Modelling* **189**:25–48.

Thuiller, W., C. Albert, M. B. Araujo, P. M. Berry, M. Cabeza, A. Guisan, T. Hickler, G. F. Midgley, J. Paterson, F. M. Schurr, et al., 2008. Predicting global change impacts on plant species' distributions: future challenges. *Perspectives in Plant Ecology, Evolution and Systematics* **9**:137–152.

Todd-Brown, K., J. Randerson, W. Post, F. Hoffman, C. Tarnocai, E. Schuur, and S. Allison, 2013. Causes of variation in soil carbon simulations from cmip5 Earth system models and comparison with observations. *Biogeosciences* **10**:1717–1736.

Vereecken, H., A. Schnepf, J. W. Hopmans, M. Javaux, D. Or, T. Roose, J. Vanderborght, M. Young, W. Amelung, M. Aitkenhead, et al., 2016. Modeling soil processes: Review, key challenges, and new perspectives. *Vadose zone journal* **15**.

Watt, A. S., 1947. Pattern and process in the plant community. *Journal of ecology* **35**:1–22.

Wikle, C. K., 2003. Hierarchical Bayesian models for predicting the spread of ecological processes. *Ecology* **84**:1382–1394.

Williams, M., P. A. Schwarz, B. E. Law, J. Irvine, and M. R. Kurpius, 2005. An improved analysis of forest carbon dynamics using data assimilation. *Global Change Biology* **11**:89–105.

Wramneby, A., B. Smith, S. Zaehle, and M. T. Sykes, 2008. Parameter uncertainties in the modelling of vegetation dynamics—effects on tree community structure and ecosystem functioning in european forest biomes. *Ecological Modelling* **216**:277–290.

Xia, Y., K. Mitchell, M. Ek, J. Sheffield, B. Cosgrove, E. Wood, L. Luo, C. Alonge, H. Wei, J. Meng, et al., 2012. Continental-scale water and energy flux analysis and validation for the North American Land Data Assimilation System project phase 2 (NLDAS-2): 1. intercomparison and application of model products. *Journal of Geophysical Research: Atmospheres* **117**.

Zaehle, S., S. Sitch, B. Smith, and F. Hatterman, 2005. Effects of parameter uncertainties on the modeling of terrestrial biosphere dynamics. *Global Biogeochemical Cycles* **19**.

Zwart, J., Z. Hanson, J. Read, M. Fienen, A. Hamlet, D. Bolster, and S. Jones, 2019. Cross-scale interactions dictate regional lake carbon flux and productivity response to future climate. *Geophysical Research Letters* **46**:8840–8851.

Part I

Supplemental Materials

5 Meterological Climate Ensemble Weights

5.1 Statistical filtering of downscaled general circulation climate model output

In this section, we outline the procedure to filter the downscaled general circulation model (GCM) output to be consistent with gridded statistical paleoclimate reconstructions. The climate products that we use for filtering are the Mann et al. (2009) reconstruction of mean annual temperature and the Living Blended Drought Atlas (LBDA) from Cook et al. (2010) for mean annual Palmer Drought Severity Index (PDSI). The Mann et al. (2009) data product contains mean temperature estimates starting in AD 500 and ending in AD 2005 at a grid-cell resolution of $5^\circ \times 5^\circ$ covering much of the globe. The Cook et al. (2010) data product contains mean annual PDSI estimates starting in AD 0 and ending in AD 2006 at a grid cell resolution of $0.5^\circ \times 0.5^\circ$ covering much of North America.

5.2 Proposed Model

The goal of the analysis is to produce a vector of weights for each member of the climate model ensemble for each year in the period 0 AD - 2000 AD. Let the empirical observations for year t be $\mathbf{y}_t = (T_t, PDSI_t)'$ where T_t is the Mann mean temperature estimate and $PDSI_t$ is the LBDA mean estimate at the grid cell of interest for year t. For the ith climate model run out of an ensemble of N different climate runs, let $\mathbf{x}_{it} = \left(\tilde{T}_{it}, \widetilde{PDSI}_{it}\right)'$ be the climate model estimate of mean annual temperature and mean annual PDSI for the grid cell of interest for year t. Then, the goal is to find weights $\mathbf{w}_t = (w_{1t}, \ldots, w_{Nt})'$ that minimize the squared difference

$$\underset{\mathbf{w}_t}{\operatorname{argmin}} \left\| \mathbf{y}_t - \sum_{i=1}^{N} w_{it}\mathbf{x}_{it} \right\|^2, \tag{10}$$

subject to the constraint that $\sum_{i=1}^{N} w_{it} = 1$. A primary goal for performing a statistical data assimilation is the preservation of variability in the weighted climate model ensemble. Model (10) has a significant issue in that the weight vector $\mathbf{w}_t$ could place very large weight on a single realization or a small handful of realizations. This is especially likely if the empirically estimated climate state is not close to the climate model ensemble. If this occurs, there will be an undesirable reduction in the variability of the weighted climate

model ensemble. One way to preserve the variability in the weighted climate model ensemble is to bootstrap the empirical climate realizations using predictive standard deviations. For example, let $\mathbf{y}_t^{(k)}$ be the kth bootstrap draw from the predictive distribution $\left[\mathbf{y}_t^{(k)} \middle| \mathbf{y}_t, \mathbf{\Sigma}_{y_t}\right]$, where $\mathbf{\Sigma}_{y_t} = \text{diag}\left(\sigma^2_{T_t}, \sigma^2_{PDSI_t}\right)$ is the predictive covariance that is assumed to be diagonal and is estimated by comparing the reconstruction predictions to the observation-era records during the modern period. Ideally, the predictive standard deviations would be included in the data product and would increase further back in time as the amount of empirical proxy data used in the reconstruction products decreases; however, the predictive standard deviations are not reported as part of the data products used. Despite this, the predictive standard deviations can be approximated by comparing the output of modern-era data products to the Mann et al. (2009) and Cook et al. (2010) empirical paleoclimate proxy products. The modern-era climate proxies used in estimating the predictive standard deviations are the parameter-elevation regression on independent slopes model (PRISM Climate Group, Oregon State University 2004) product for mean annual temperature and the annual mean PDSI data product from Dai, Trenberth, and Qian (2004)[1] where we extract the record at the location of interest during the period of overlap in the modern era and calculate the root mean sum of squares as an estimate of the predictive standard deviation. In truth, one would expect these uncertainties to increase further in the past as paleoclimate data used to fit the models becomes more sparser; however, we treat these as constant in time as a first order approximation. Then, applying Eq. (10) to each of the bootstrap samples (assuming a Gaussian predictive distribution) produces a bootstrap distribution of weights $\mathbf{w}_t^{(k)}$ and the final weighted model ensemble is given by the bootstrap-averaged weights

$$\bar{\mathbf{w}}_t = \frac{1}{K}\sum_{k=1}^{K} \underset{\mathbf{w}_t^{(k)}}{\text{argmin}} \left\| \mathbf{y}_t^{(k)} - \sum_{i=1}^{N} w_{it}^{(k)} \mathbf{x}_{it} \right\|^2 . \tag{11}$$

Thus, the bootstrap-averaged weights show less degeneracy and do a better job of preserving the variability in the weighted model ensemble.

[1] Dai Palmer Drought Severity Index data provided by the NOAA/OAR/ESRL PSD, Boulder, Colorado, USA, from their Web site at `https://www.esrl.noaa.gov/psd/`

6 Prior Distributions

6.1 Red Maple Prior Distributions

	distn	parama	paramb	n
SLA	weibull	0.50	10.00	2548
DMAX	norm	6600.00	1.00	
DMIN	norm	1000.00	1.00	
AGEMX	unif	100.00	200.00	
SPRTND	norm	13.00	1.00	
SPRTMX	norm	200.00	1.00	
D3	unif	0.25	0.75	
CM1	unif	2.69	2.89	
CM2	norm	219.77	1.00	
CM3	unif	0.00	0.00	
CM4	norm	-0.60	0.10	
CM5	norm	0.85	0.10	
FWT	unif	400.00	480.00	
Gmax	norm	100.00	1.00	
MPLANT	lnorm	4.45	1.00	
FROST	norm	-17.00	2.00	
SLTA	norm	0.01	0.25	
SLTB	norm	0.37	0.25	
HTMAX	norm	15.00	1.00	
DBHMAX	norm	0.86	0.03	

Table 5: Red Maple Prior Distributions

6.2 Yellow Birch Prior Distributions

	distn	parama	paramb	n
SLA	weibull	0.50	10.00	2548
DMIN	norm	1100.00	1.00	
HTMAX	norm	30.00	1.00	
DBHMAX	norm	0.80	0.03	
AGEMX	unif	150.00	350.00	
Gmax	norm	50.00	1.00	
SPRTND	norm	43.00	1.00	
SPRTMX	norm	100.00	1.00	
SPRTMN	norm	12.00	1.00	
D3	unif	0.25	0.75	
FWT	unif	200.00	300.00	
CM1	unif	2.84	3.04	
CM2	norm	117.52	1.00	
CM3	unif	0.00	0.00	
CM4	norm	-1.20	0.10	
CM5	norm	1.30	0.10	
DMAX	norm	2500.00	1.00	
MPLANT	lnorm	6.83	1.00	
FROST	norm	-18.00	2.00	
SLTA	norm	0.07	0.25	
SLTB	norm	0.01	0.25	

Table 6: Yellow Birch Prior Distributions

6.3 Beech Prior Distributions

	distn	parama	paramb	n
SLA	weibull	0.50	10.00	2548
DMIN	norm	1326.00	50.00	
AGEMX	weibull	2.00	494.97	
Gmax	unif	52.00	92.00	
SPRTND	norm	172.00	1.00	
SPRTMX	norm	30.00	1.00	
MPLANT	unif	0.00	60.00	
HTMAX	norm	30.00	1.00	
DBHMAX	lnorm	1.00	1.00	
D3	unif	0.25	0.75	
FWT	unif	400.00	480.00	
CM1	unif	2.84	3.04	
CM2	norm	117.52	1.00	
CM3	unif	0.00	0.00	
CM4	norm	-1.20	0.10	
CM5	norm	1.30	0.10	
root2shoot	beta	1.00	1.00	
DMAX	norm	5537.00	10.00	
FROST	unif	-100.00	0.00	
SPRTMN	norm	6.00	1.00	
SLTA	norm	0.57	0.25	

Table 7: Beech Prior Distributions

6.4 Red Oak Prior Distributions

	distn	parama	paramb	n
SLA	weibull	0.50	10.00	2548
D3	unif	0.25	0.75	
FWT	unif	400.00	480.00	
CM1	unif	2.84	3.04	
CM2	norm	117.52	1.00	
CM3	unif	0.00	0.00	
CM4	norm	-1.20	0.10	
CM5	norm	1.30	0.10	
DMAX	norm	4571.00	1.00	
DMIN	norm	1100.00	1.00	
AGEMX	unif	300.00	500.00	
Gmax	norm	130.00	1.00	
SPRTND	norm	32.00	1.00	
SPRTMX	norm	40.00	1.00	
SPRTMN	norm	17.00	1.00	
MPLANT	lnorm	2.64	1.00	
FROST	norm	-18.00	2.00	
SLTA	norm	-0.30	0.25	
SLTB	norm	0.52	0.25	
HTMAX	norm	48.00	1.00	
DBHMAX	norm	1.50	0.03	

Table 8: Red Oak Prior Distributions

6.5 Hemlock Prior Distributions

	distn	parama	paramb	n
SLA	weibull	0.50	10.00	2548
DMIN	norm	1324.00	10.00	
HTMAX	unif	30.00	40.00	
DBHMAX	unif	1.00	2.00	
AGEMX	weibull	2.00	1060.66	
Gmax	unif	27.00	67.00	
D3	unif	0.25	0.75	
CM1	unif	2.69	2.89	
CM2	norm	219.77	1.00	
CM3	unif	0.00	0.00	
CM4	norm	-0.60	0.10	
CM5	norm	0.85	0.10	
FWT	unif	400.00	480.00	
root2shoot	beta	1.00	1.00	
DMAX	norm	3800.00	10.00	
MPLANT	lnorm	6.58	1.00	
FROST	norm	-13.00	2.00	
SLTA	norm	-0.02	0.25	
SLTB	norm	0.36	0.25	

Table 9: Hemlock Prior Distributions

6.6 Parameter Uncertainty Analysis Results

We also found that climate related parameters related to growing degree day minimum and maximum and frost tolerance were causing LINKAGES to consider some species not viable for growth. For these climate envelope parameters we expanded the priors to include values within the range of our meteorological data centered on the LINKAGES default parameter values. We found that parameters affecting total aboveground biomass sensitivity varied between species (Figure 11). Red maple biomass is most sensitive to nitrogen growth multiplier 1 (CM1) and somewhat sensitive to maximum seeding rate per plant (MPLANT). Yellow birch and beech are most sensitive to number of sprouts per stump (SPTRND). Red oak has the most sensitive to nitrogen growth multiplier 2 (CM2).

Figure 11: Partial variance of LINKAGES 21 species specific parameters calculated from full sensitivity analysis on output variable total aboveground biomass.

7 Ecosystem Model Restart

Once we have obtained the updated state variable matrix, we needed to restart our ecosystem model by rewriting the state variables into ecosystem model specific formats. For LINKAGES, we calculate new species density and individual tree DBHs so that the stand level biomass estimated in the MCEnF matches LINKAGES individual biomass calculations. To do this we first calculate each individual tree's forecast biomass and aggregate this to a species level. We determine a biomass correction factor by dividing the

updated biomass from the MCEnF by the species biomass from the LINKAGES forecast. Then, we sample from the original pool of individuals based off the analysis biomass to obtain a new number of individuals. Adjusting the species level tree density first allows us to preserve stand age and size distribution from LINKAGES. Next, we adjust the individual's DBH directly using an optimization function to match the stand level biomass given from the MCEnF analysis. Soil carbon is much less complicated in LINKAGES, so we apply a soil carbon correction factor directly. These new model specific state variables are fed back into LINKAGES as current state variables.

8 Species Bias Diagnostics

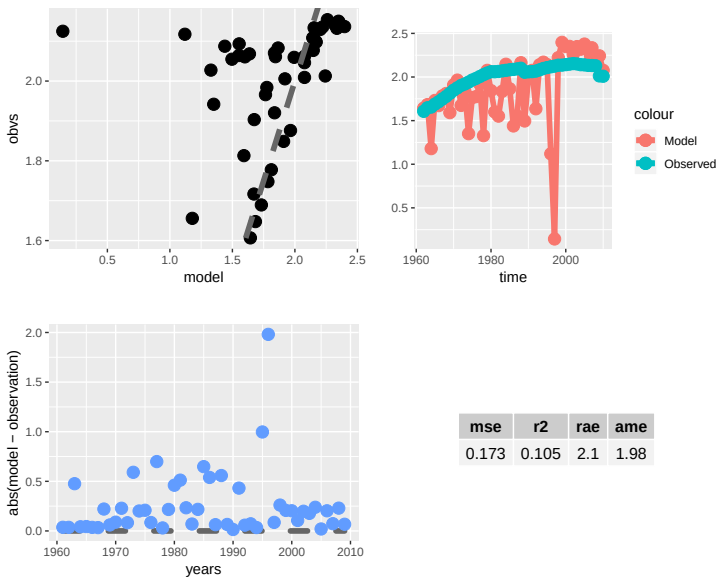

mse	r2	rae	ame
0.173	0.105	2.1	1.98

Figure 12: Bias diagnostics for red maple

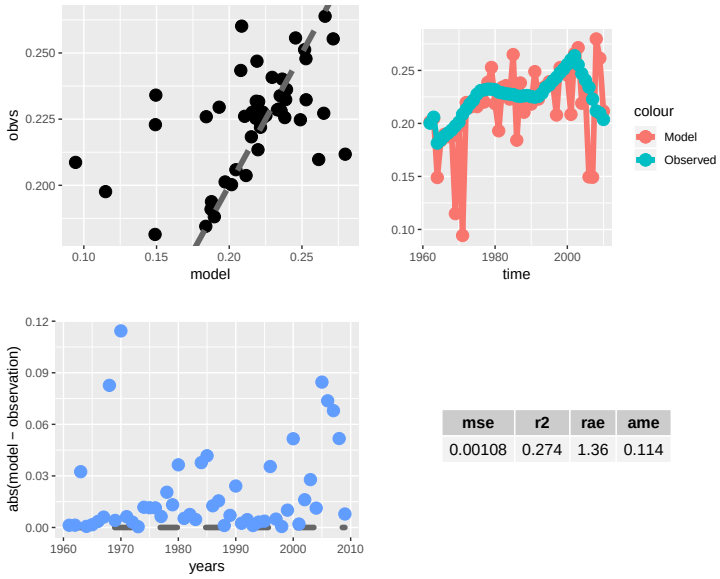

mse	r2	rae	ame
0.00108	0.274	1.36	0.114

Figure 13: Bias diagnostics for yellow birch

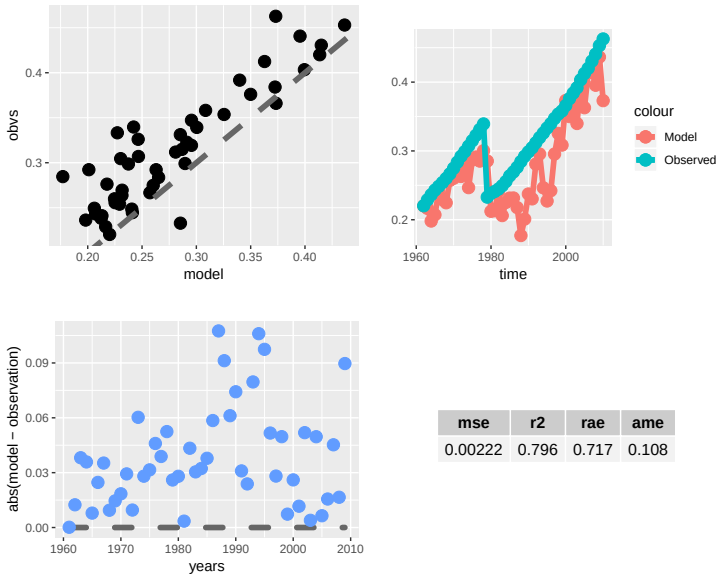

mse	r2	rae	ame
0.00222	0.796	0.717	0.108

Figure 14: Bias diagnostics for American beech

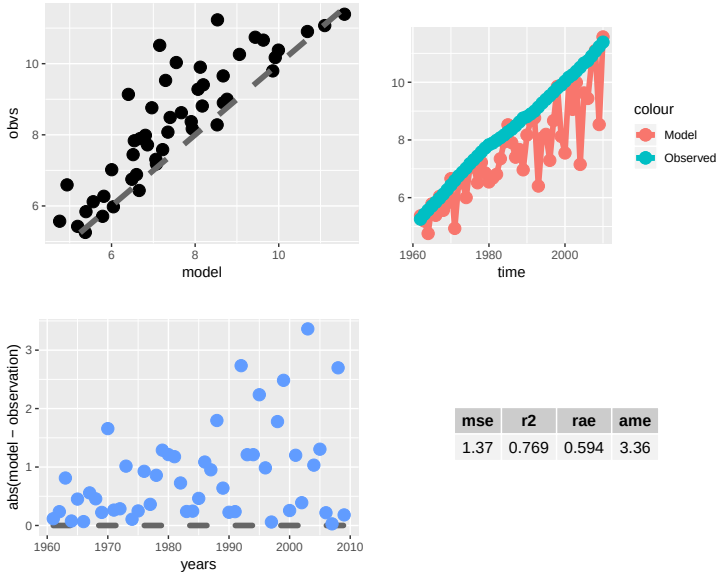

mse	r2	rae	ame
1.37	0.769	0.594	3.36

Figure 15: Bias diagnostics for red oak

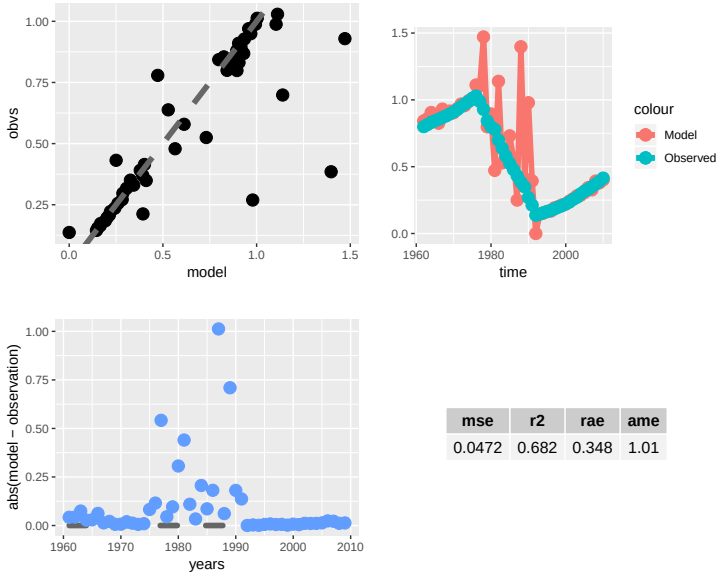

mse	r2	rae	ame
0.0472	0.682	0.348	1.01

Figure 16: Bias diagnostics for eastern hemlock

9 Spin IC Species Level

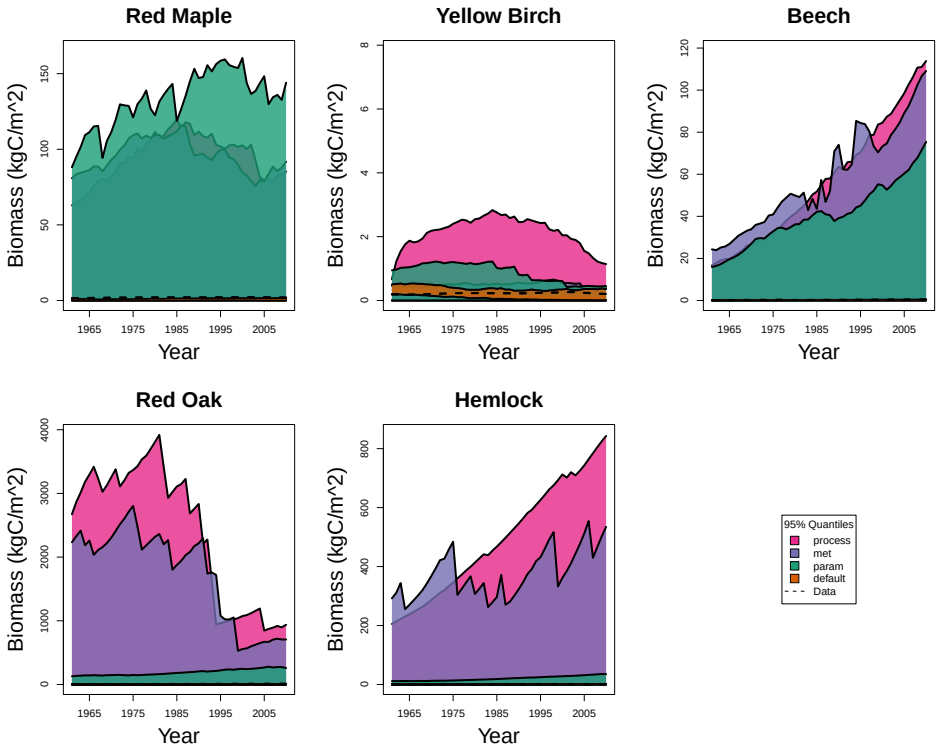

Figure 17: 95% quantiles of species level biomass over time colored by the four data spin up initial condition uncertainty scenarios (scenarios A1-4). Variance from the first scenario arises only from demographic stochasticity (orange). Parameter, meteorological, and process uncertainty are added sequentially in the next three scenarios where the fourth scenario, with the widest credible intervals, contains variance from demographic stochasticity, parameters, meteorology, and process uncertainties. The dotted lines on all the plots are the 95% credible intervals of the data estimated from tree rings.

10 Forecast Covariance

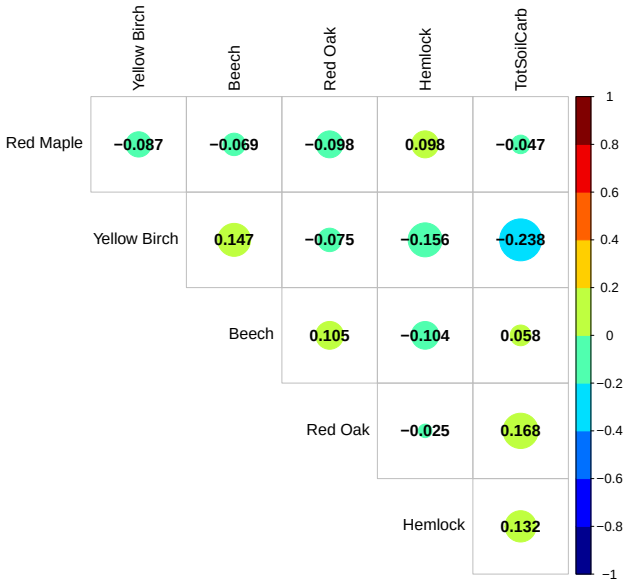

Figure 18: Correlations between species level biomass from the LINKAGES forecast.